AD-A054 286 WESTINGHOUSE DEFENSE AND ELECTRONIC SYSTEMS CENTER B--ETC F/G 14/2
LIGHTWEIGHT LINE PULSER.(U)
APR 78 H J BLINCHIKOFF F30602-76-C-0207
UNCLASSIFIED 78-0099 RADC-TR-78-73 NL

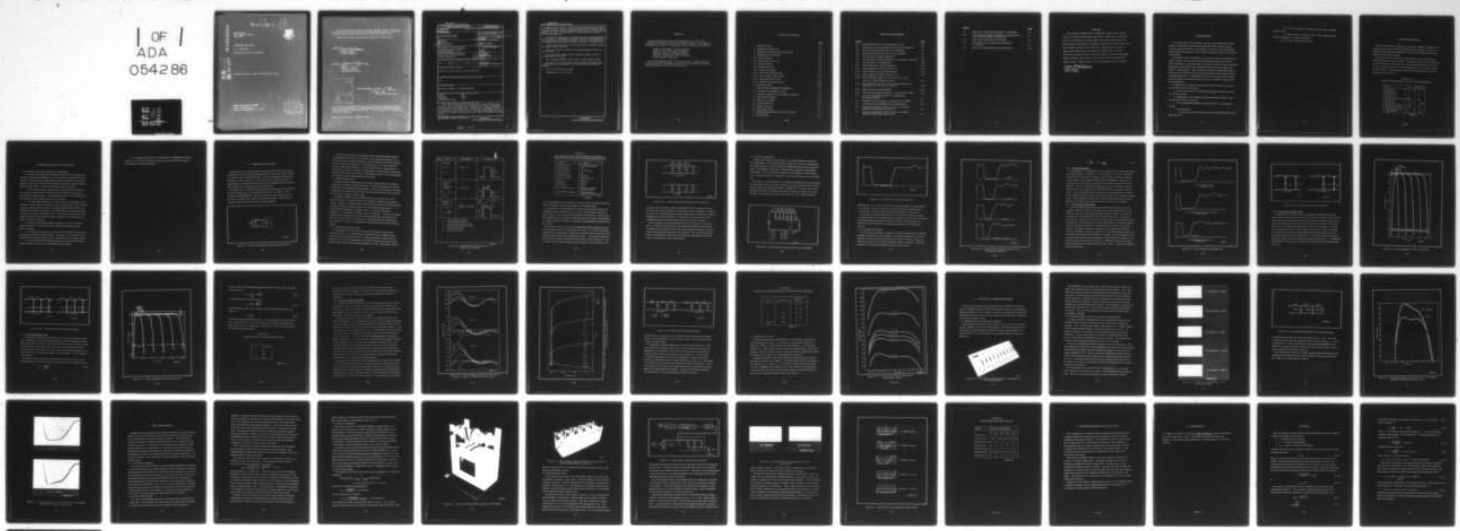

1 OF 1
ADA
054286

END
DATE
FILMED
6-78
DDC

RADC-TR-78-73
Final Technical Report
April 1978

LIGHTWEIGHT LINE PULSER

H. J. Blinchikoff

Westinghouse Electric Corporation

ROME AIR DEVELOPMENT CENTER
Air Force Systems Command
Griffiss Air Force Base, New York 13441

This report has been reviewed by the RADC Information Office (OI) and is releasable to the National Technical Information Service (NTIS). At NTIS it will be releasable to the general public, including foreign nations.

RADC-TR-78-73 has been reviewed and is approved for publication.

APPROVED: James VanDamme
JAMES VANDAMME
Project Engineer

APPROVED: Joseph L Ryerson
JOSEPH L. RYERSON
Technical Director
Surveillance Division

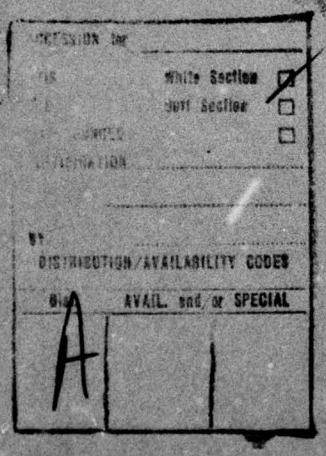

FOR THE COMMANDER: John P. Huss
JOHN P. HUSS
Acting Chief, Plans Office

If your address has changed or if you wish to be removed from the RADC mailing list, or if the addressee is no longer employed by your organization, please notify RADC (OCTP), Griffiss AFB NY 13441. This will assist us in maintaining a current mailing list.

Do not return this copy. Retain or destroy.

UNCLASSIFIED

SECURITY CLASSIFICATION OF THIS PAGE (When Data Entered)

REPORT DOCUMENTATION PAGE

READ INSTRUCTIONS BEFORE COMPLETING FORM

1. REPORT NUMBER: RADC-TR-78-73	2. GOVT ACCESSION NO.
3. RECIPIENT'S CATALOG NUMBER	
4. TITLE (and Subtitle): LIGHTWEIGHT LINE PULSER	5. TYPE OF REPORT & PERIOD COVERED: Final Technical Report. 1 May 76 - 1 Dec 77
6. PERFORMING ORG. REPORT NUMBER: 78-0099	
7. AUTHOR(s): Herman R. J. Blinchikoff	8. CONTRACT OR GRANT NUMBER(s): F30602-76-C-0207
9. PERFORMING ORGANIZATION NAME AND ADDRESS: Westinghouse Electric Corporation, Systems Development Division, Baltimore MD 21203	10. PROGRAM ELEMENT, PROJECT, TASK AREA & WORK UNIT NUMBERS: 62702F, 45060366
11. CONTROLLING OFFICE NAME AND ADDRESS: Rome Air Development Center (OCTP), Griffiss AFB NY 13441	12. REPORT DATE: April 1978 13. NUMBER OF PAGES: 55 p.
14. MONITORING AGENCY NAME & ADDRESS (if different from Controlling Office): Same	15. SECURITY CLASS (of this report): UNCLASSIFIED 15a. DECLASSIFICATION/DOWNGRADING SCHEDULE: N/A

16. DISTRIBUTION STATEMENT (of this Report)

Approved for public release; distribution unlimited

17. DISTRIBUTION STATEMENT (of the abstract entered in Block 20, if different from Report)

Same

18. SUPPLEMENTARY NOTES

RADC Project Engineer: James VanDamme (OCTP)

19. KEY WORDS (Continue on reverse side if necessary and identify by block number)

Module
Modulator
Lightweight
Pulse Forming Network
PFN
Pulser
Radar

20. ABSTRACT (Continue on reverse side if necessary and identify by block number)

This report describes the work performed under contract F30602-76-C-0207 to study, develop, and demonstrate the feasibility of a compact, lightweight, modular, pulse-forming network (PFN). The PFN evolved is composed of identical LC modules and an input module that is optimized for a pulse-plateau ripple that satisfies the goal of ± 0.5 percent. The ripple remains within this limit as modules are added or removed from the PFN to change the pulsewidth in 2 μsec steps.

DD FORM 1 JAN 73 1473 EDITION OF 1 NOV 65 IS OBSOLETE

UNCLASSIFIED

SECURITY CLASSIFICATION OF THIS PAGE (When Data Entered)

405 897

This low-ripple response is achieved without incorporating mutual inductance into the design, therefore, easing the module tuning and assembly. Mutual inductance has been considered indispensible in PFN's, but it is a roadblock for modular construction. Its elimination as a design parameter is the key to realizing the modular PFN.

All electrical design goals are satisfied and the size goal was achieved by a wide margin. The realized volume energy density of 0.1 joules/in^3 was the best achievable with off-the-shelf capacitors. The goal of 0.5 joules/in^3 is not compatible with present state-of-the-art components at these power levels.

Included herein are results of the following studies undertaken to satisfy the original contract objectives:

Theoretical analysis of distributed and lumped constant lines that can realize the PFN.

Optimization of the lumped-constant network that yields a pulse-top variation within $\pm$ 0.5 percent.

Test of breadboard modules using low power to verify modular concept.

Investigation of capacitor types, coil construction, and modular design to minimize size, obtain ruggedness, and allow easy addition or removal of modules.

Test of final PFN under full power.

Recommendations for future study.

PREFACE

This Final Report describes work performed from 1 May 1976 to 1 December 1977 under Contract No. F30602-76-C-0207. The report was compiled by Dr. Herman J. Blinchikoff. Project staffing was as follows:

Robert A. Gardenghi - Program Manager
Robert A. Hill - Principle Investigator
Edward H. Hooper - Technical Advisor
Herman J. Blinchikoff - Network Analysis
S. Ivan Rambo - Consultant

The author wishes the thank J. Van Damme and F. Welker of the U.S. Air Force Rome Air Development Center for their support and valuable suggestions during the course of this program.

TABLE OF CONTENTS

	Page
1. INTRODUCTION	1-1
2. PROGRAM OBJECTIVE	2-1
3. IMPORTANT RESULTS OF THIS STUDY	3-1
4. THEORETICAL ANALYSIS	4-1
4.1 Distributed Line	4-2
4.2 Lumped Parameter Line	4-2
4.3 Type E Networks	4-6
4.4 Rayleigh Networks	4-7
4.4.1 Initial Investigation	4-9
4.4.2 Two-Section Module Study	4-9
4.4.3 Three-Section Module Study	4-11
4.4.4 Perturbation Rise Time	4-13
4.4.5 Optimum Rayleigh Network	4-16
4.5 Sensitivity Study	4-20
5. LOW-POWER BREADBOARD MODELS	5-1
5.1 Verification of Modular Concept	5-1
5.2 Optimum Design and Lead Length Investigation	5-2
6. HIGH POWER MODEL	6-1
6.1 Capacitor Assembly	6-1
6.2 Coil Construction	6-1
6.3 Module Assembly	6-1
6.4 High-Power Tests	6-1
7. RECOMMENDATIONS FOR FUTURE STUDY	7-1
8. REFERENCES	8-1

LIST OF ILLUSTRATIONS

Figure		Page
4-1	Equivalent Model for Pulse Discharge Current	4-1
4-2	Distributed Line Performance for Three Loss Conditions	4-3
4-3	Pulse Forming Networks That Were Examined	4-5
4-4	Six-Section Type E PFN with 10 μsec Pulsewidth	4-6
4-5	Current Pulse of PFN in Figure 4-4	4-7
4-6	Current Pulses of PFN in Figure 4-4 as Sections are Removed	4-8
4-7	Current Pulses of Rayleigh PFN	4-10
4-8	Two-Section Pulse Forming Modules	4-11
4-9	Pulse Responses of PFN in Figure 4-8	4-12
4-10	Three-Section Pulse Forming Modules	4-13
4-11	Pulse Responses of PFN in Figure 4-10	4-14
4-12	Pulse Responses About The Pulse Top As L_1 and C_1 Vary (N = 3 PFM in Figure 4-10(a))	4-17
4-13	Pulse Responses for One, Two, and Three Modules for Optimum L_1 (3.4 μH) and C_1 (0.073 μF)	4-18
4-14	Optimum Pulse Forming Modules	4-19
4-15	Pulse Forming Module Response as Load Resistor Varies	4-21
5-1	Low-Power Breadboard PFN for Verification of Theoretical Results	5-1
5-2	Response of PFN in Figure 5-1 as Sections are Added	5-3
5-3	Two Microsecond Optimum Pulse Forming Module	5-4
5-4	Computed Responses of PFN in Figure 5-3 Including Capacitor Lead Length Inductance L_x	5-5
5-5	Measured Responses of PFN in Figure 5-4 Including Capacitor Lead Length Inductance L_x	5-6

Figure		Page
6-1	High-Power Pulse Forming Module - Final Model	6-4
6-2	Pulse Forming Network Realized as a Cascade of the Pulse Forming Modules in Figure 6-1	6-5
6-3	High-Power Test Circuit for the PFM	6-6
6-4	Low-Power Pulse Responses of Final PFN's (1 μsec/cm)	6-7
6-5	High-Power Pulse Responses of Final PFN's	6-8

EVALUATION

This program has demonstrated a lightweight, modular pulse forming network for radar and other pulse applications. Modularity, an important factor in serviceability and ECCM pulse width agility applications, has been achieved through the use of identical modules with no mutual inductance, thus eliminating tuning of the entire PFN. Modules may be serviced for longer pulse lengths and/or paralleled for greater power. With the appropriate switching circuits, this can be done on a pulse-to-pulse basis. Ripple, overshoot, and droop are less than one percent for excellent RF signal fidelity. Weight density of 5.12 J/LB exceeds the goal of 2J/LB.

James M VanDamme

JAMES VANDAMME
Project Engineer

1. INTRODUCTION

This report describes the design, analysis, and realization of a lightweight, low impedance pulse-forming network (PFN) in which identical inductor-capacitor modules can be added or removed to change pulsewidth while maintaining high pulse quality without introducing excessive pulse-top perturbations.

The need for this type of PFN arises from the growing sophistication of modern tactical radars, particularly transportable radars with modern ECCM capabilities. Advanced signal processing techniques require improved transmitter pulse fidelity, which depends heavily on the modulator pulse quality. Furthermore, a radar requirement exists for pulsewidth agility in which line type modulators may be made pulsewidth variable through the use of modularized PFN's. Conventional PFN's are heavy and bulky, and the pulse-top ripple associated with these devices is considered excessive for these applications.

The effort on this program to develop the PFN described in section 2 was divided into five major parts.

a. Theortical analysis of distributed and lumped constant lines that can realize the PFN.

b. Optimization of the lumped-constant network that yields a pulse-top variation within ± 0. 5 percent.

c. Test of breadboard modules using low power to verify modular concept.

d. Investigation of:

(1) Capacitor types to determine the one most applicable for the lightweight PFN.

(2) Coil construction to minimize size and reduce coupling between coils.

(3) Module design to minimize size, obtain ruggedness and allow easy addition or removal of modules.

e. Test of final PFN under full power.

2. PROGRAM OBJECTIVE

The objective of this program was to develop a compact, lightweight, low impedance pulse-forming module (PFM) that can be added or removed to lengthen or decrease the pulsewidth of a given system without introducing excessive pulse-plateau ripple.

In the context of this report, the pulse-forming network (PFN) is the aggregate of pulse-forming modules. The pulse duration of each PFM is to be 2 microseconds. Therefore, the pulse duration of the PFN can be 2, 4, 6, 8, or 10 microseconds, since the maximum number of modules considered here is five. The parameter goals for the PFM and the achieved results are given in table 2-1.

TABLE 2-1

PULSE-FORMING MODULE GOALS AND ACHIEVEMENTS

Parameter	Goal	Achievement
Peak Power (mW)	5	5
Average Power (kW)	4	4
Charging Voltage (kV)	10	10
Pulse Duration (μsec)	2	2
Pulse Repetition Frequency (pps)	400 max	400
Impedance (ohms)	5	5
Pulse-Top Variation	1% max	1% max
Weight Energy Density (joules/lb)	2 min	5.1
Volume Energy Density (joules/in^3)	0.5 min	0.1
Max Dimension for Stack of 5 Modules (inches)	60	17.8

78-0099-TA-1

3. IMPORTANT RESULTS OF THIS STUDY

The important results of this study are stated below.

a. We have realized a PFN composed of identical LC modules, and an input module that is optimized for a pulse-plateau ripple less than ± 0. 5 percent. This theoretical ripple remains within the goal of ± 0. 5 percent as these modules are added or removed from the PFN to change the pulse-width in 2 μsec steps. All electrical design goals are satisfied.

b. The measured plateau ripple of the PFN high-power model was ± 1. 5 percent, achieved with components whose tolerance was within ± 5 percent of the nominal values. The design goal of ± 0. 5 percent ripple will be satisfied as this component tolerance is improved.

c. The low-ripple response is achieved without incorporating mutual inductance into the design, therefore, easing the module tuning and assembly. Until now, mutual inductance has been indispensible in PFN's, but it is a roadblock for modular construction. Its elimination as a design parameter is the key to realizing the modular PFN. The absence of necessary mutual suggests that the network inductors might be wound on the capacitors as a means to reduce overall size.

d. The use of paper-polypropylene capacitors results in a weight energy density of 5. 1 joules per pound, bettering the design goal of 2 joules per pound.

e. The realized volume energy density of 0. 1 joules/in^3 was the best achievable with off-the-shelf capacitors. The goal of 0. 5 joules/in^3 is not compatible with present state-of-the-art components at these power levels.

f. We have shown that the distributed line is not a practical realization for this PFN because of size and weight considerations.

g. The optimum parameters are presented in normalized form (paragraph 4.4.5) allowing the optimum response to be achieved for arbitrary pulsewidths and network impedances.

4. THEORETICAL ANALYSIS

The PFN serves the dual purpose of storing the exact amount of energy required for a single pulse and discharging this energy into a load resistor R_o in the form of a rectangular pulse. An equivalent model for this pulse discharge is shown in figure 4-1, where the PFN is selected so that i(t) approximates a rectangular pulse to within an acceptable tolerance when the input voltage v(t) is the step function of amplitude E.

The ideal PFN is an open-circuited lossless transmission line of characteristic impedance $Z_o = R_o$ and transmission time $\tau/2$, where τ is the rectangular pulsewidth [1]. However, practical considerations rule out this line as a PFN, and in practice this distributed line is simulated by a network composed of a finite number of lump elements.

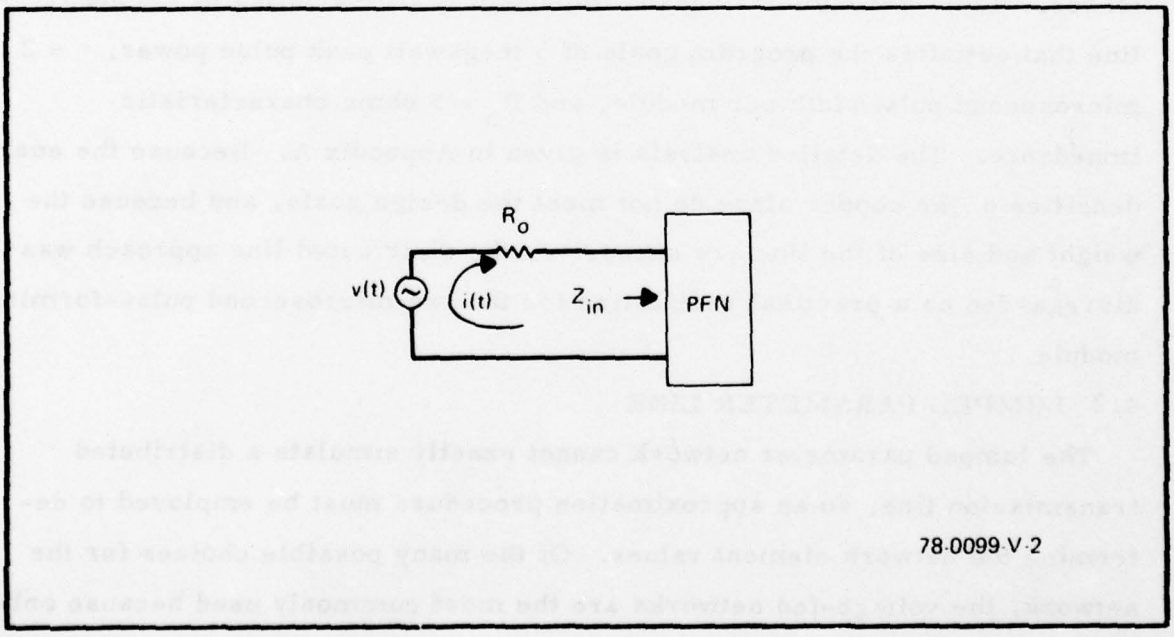

Figure 4-1. Equivalent Model for Pulse Discharge Current

Our theoretical analysis was divided into two separate parallel efforts. The distributed parameter line, because of its apparent advantages of construction ease and compact packaging, was investigated and its shortcomings are described in paragraph 4.1. In paragraph 4.2 we review classical lumped constant approximations to the distributed line, in paragraph 4.3 we discuss the Type E networks, in paragraph 4.4 we describe our approach that led to the final element values of the optimized PFN, and in paragraph 4.5 the sensitivity of the optimum PFN is discussed.

4.1 DISTRIBUTED LINE

Although the ideal transmission line yields a flat-top pulse, unavoidable conduction or dielectric losses in the line cause pulse dispersion in the line and droop on the resulting discharge pulse. Figure 4-2 summarizes the pulse outputs for the lossless line, the lossy line with constant attenuation, and the lossy line with conductive losses only.

A realistic condition for the transmission line is given by Case III in figure 4-2; that is, dielectric losses are negligible compared to conduction losses. Table 4-1 summarizes the important characteristics of the distributed line that satisfies the program goals of 5 megawatt peak pulse power, $\tau = 2$ microsecond pulsewidth per module, and $R_o = 5$ ohms characteristic impedance. The detailed analysis is given in Appendix A. Because the energy densities of the copper alone do not meet the design goals, and because the weight and size of the line are excessive, the distributed line approach was disregarded as a practical realization for the two microsecond pulse-forming module.

4.2 LUMPED PARAMETER LINE

The lumped parameter network cannot exactly simulate a distributed transmission line, so an approximation procedure must be employed to determine the network element values. Of the many possible choices for the network, the voltage-fed networks are the most commonly used because only with this type can the usual discharge switches be used. The energy, stored

Case	Conditions	Input Impedance, Z_{in}	Current Pulse, i(t)
I	Lossless Line $R = G = 0$ $Z_o = R_o$	$R_o \coth \frac{\tau}{2} s$	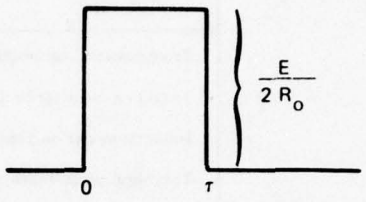
II	Lossy Line With Constant Attenuation and Linear Phase $\frac{R}{L} = \frac{G}{C} = a$ $Z_o = R_o$	$R_o \coth \frac{\tau}{2}(s+a)$	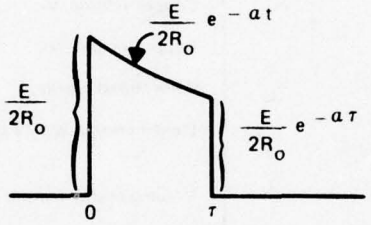
III	Conductive Losses Only, No Dielectric Losses $G = 0 \quad \frac{R}{L} = a$ $Z_o = R_o \sqrt{\frac{s+a}{s}}$	$R_o \sqrt{\frac{s+a}{s}} \coth \frac{\tau}{2} \sqrt{s(s+a)}$	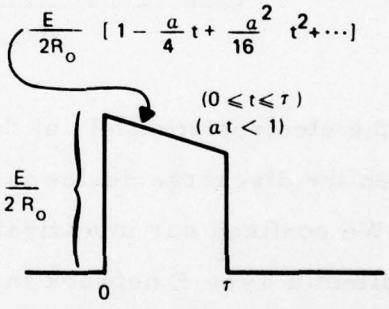

L is the series inductance per unit length

C is the shunt capacitance per unit length

R is the equivalent series resistance per unit length

G is the equivalent shunt conductance per unit length

Z_o is the characteristic impedance

R_o is the load resistance for the PFN

78-0099-V-3

Figure 4-2. Distributed line Performance for Three Loss Conditions

TABLE 4-1

TRANSMISSION LINE CHARACTERISTICS ASSUMING A 2 PERCENT DROOP ON THE TWO MICROSECOND PULSE

Parameter	Characteristic
Transmission line length, l	649 ft (polyethylene dielectric)
Total line inductance, L_T	5 μH
Inductance per unit length, L	7.7×10^{-3} μH per foot
Total line capacitance, C_T	0.2 μF
Capacitance per unit length, C	308 pF per foot
Resistance per unit length, R	3.08×10^{-4} ohms per foot
Copper volume, V	0.469 cubic feet
Copper weight, W	261 pounds
Pulse stored energy, E	10 joules
Weight energy density of copper only	0.038 joules per pound (design goal = 2 joules per pound)
Volume energy density of copper only	0.0124 joules per cubic inch (design goal = 0.5 joules per cubic inch)

78-0099-TA-4

in the electrostatic field of the PFN, is transferred to the load resistor R_o when the discharge device is switched to a conducting state.

We confined our investigation to two voltage-fed network classes; the Guillemin Type E network in figure 4-3(a), and the Rayleigh network in figure 4-3(b). In each network all capacitors are the same. Other equivalent networks for the Guillemin voltage-fed network are given in paragraph 6.3 of [1], but these networks do not offer any appreciable advantages over the Type E.

The network in figure 4-3(b) is the lumped-parameter approximation to the transmission line, truncated after N sections. We call it the Rayleigh network because application of Rayleigh's principle to the transmission line yields this two terminal line-simulating network. The Rayleigh network is well suited for modular separation because each section is identical. The Guillemin Type E network, because the inductors are not restricted to be

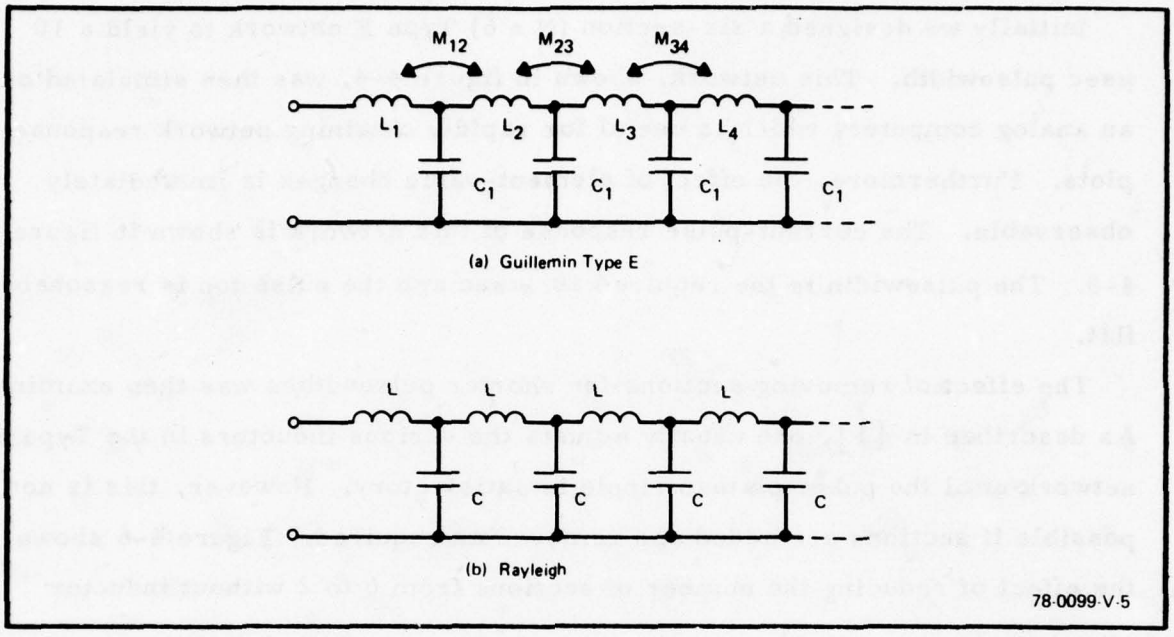

Figure 4-3. Pulse-Forming Networks That Were Examined

the same value, produces a better approximation to the rectangular pulse than does the Rayleigh network, for the same number of elements. However, the close interrelationship among element values does not make this network adaptable for modular separation. Furthermore, careful control of the coupling between coils is required to achieve the correct response.

Our investigation of lumped parameter lines was two part. In the first part, in an effort to meet the pulse-top ripple and modular requirements, we examined the responses of the Type E and Rayleigh networks as element values were changed and sections were removed. The second part was devoted to the Rayleigh network and considered the optimization of the first section to satisfy these same requirements.

4.3 TYPE E NETWORKS

Initially we designed a six-section (N = 6) Type E network to yield a 10 μsec pulsewidth. This network, shown in figure 4-4, was then simulated on an analog computer, which is useful for rapidly obtaining network response plots. Furthermore, the effect of element-value changes is immediately observable. The current-pulse response of this network is shown in figure 4-5. The pulsewidth is the required 10 μsec and the pulse top is reasonably flat.

The effect of removing sections for shorter pulsewidths was then examined. As described in [1], one usually adjusts the various inductors in the Type E network until the pulse-plateau ripple is satisfactory. However, this is not possible if sections are added and removed as required. Figure 4-6 shows the effect of reducing the number of sections from 6 to 2 without inductor

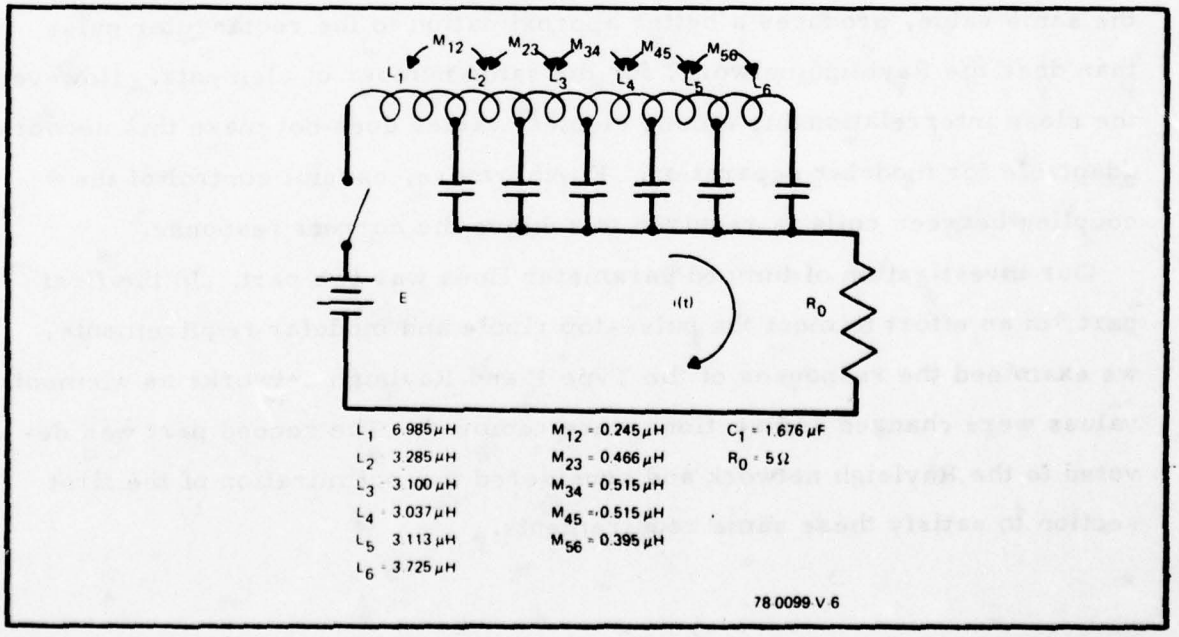

Figure 4-4. Six-Section Type E PFN With 10 μsec Pulsewidth

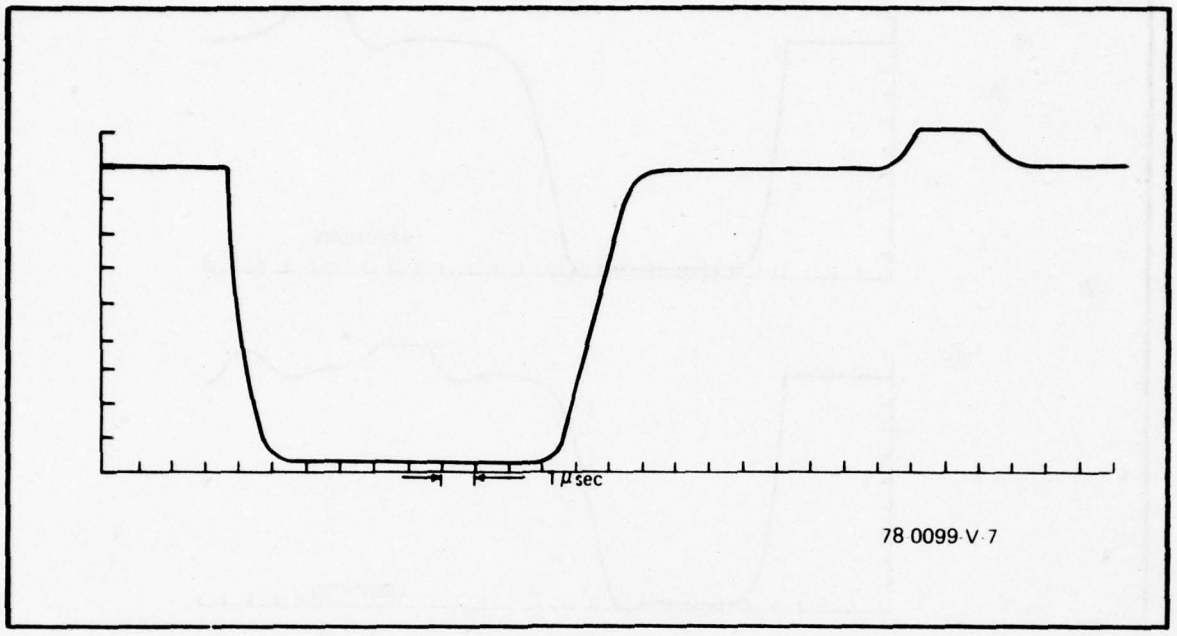

Figure 4-5. Current Pulse of PFN in Figure 4-4.

compensation. For 4 and 5 sections, the pulse-top ripple is approximately ±2.5 percent, and for 3 sections, the pulse-top ripple is approximately ±1.3 percent. All three cases do not meet the goal of ±0.5 percent.

Excessive pulse plateau distortion occurs whenever sections are added or removed because the carefully chosen aggregate of section self-inductances and mutual inductance between sections is upset. For this reason, the Type E PFN was excluded as a network that meets the requirements in section 2.

4.4 RAYLEIGH NETWORKS

The results in paragraph 4.3 suggested that the requirement of a variable pulsewidth could best be accomplished, and most economically, by having identical sections without mutual inductance between sections. The pulsewidth then becomes a function of the number of plug-in modules. This configuration is the Rayleigh network in figure 4-3(b), where

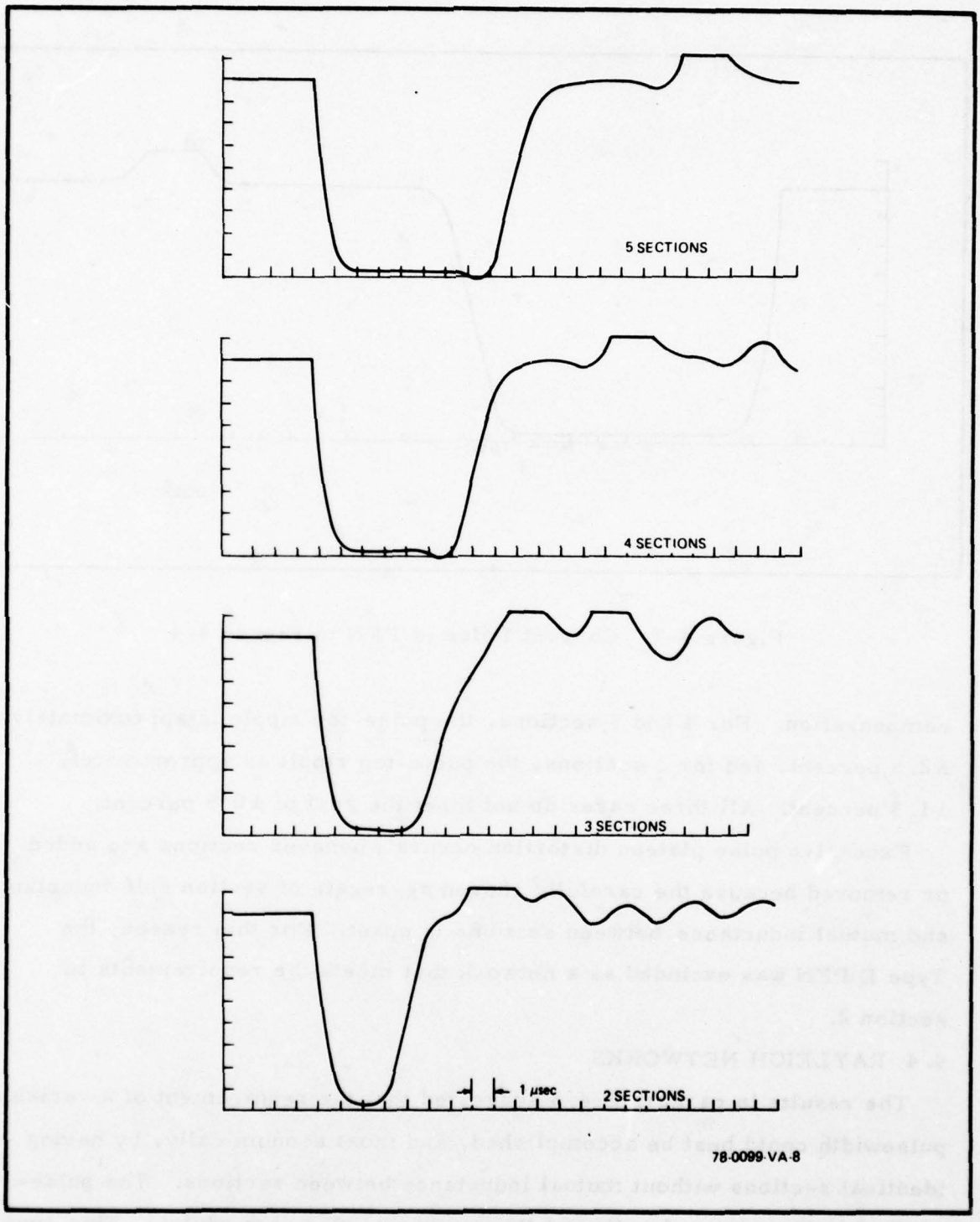

Figure 4-6. Current Pulses of PFN in Figure 4-4 as Sections are Removed

$$L = \frac{R_o \tau}{2N} , \quad C = \frac{\tau}{2NR_o} \tag{4-1}$$

4.4.1 Initial Investigation

A six-section (N = 6) Rayleigh PFN was designed for a 10 μsec pulsewidth and 5 ohm impedance, yielding L = 4.167 μH and C = 0.167 μF. The first overshoot of this network's response, shown in figure 4-7(a) is 12 percent, a figure that is unacceptable for most practical situations. However, by increasing the value of the first inductor, the response in figure 4-7(b) is obtained. The first overshoot and ripple have been considerably reduced. Then the three end sections were removed yielding the response in figure 4-7(c). The pulsewidth halved as desired and, most important, the change in the initial overshoot and rise time due to the removal of sections is insignificant. This experiment showed that a modularized PFN without mutual inductance is feasible and provided the basis for the next investigation.

4.4.2 Two-Section Module Study

First, the digital computer was programmed to calculate the current response of the PFN because accurate values of the small pulse-top variations were not obtainable from the analog computer results. Then we investigated the PFN composed of the sections in figure 4-8. The basic 2 μsec module is shown in figure 4-8(b) while the input section in figure 4-8(a) is obtained by adjusting the first inductor and capacitor of the basic module until the pulse-top variations are considerably less than the classical 12 percent. The digital computer responses of this network, as identical sections are added, are shown in figure 4-9. The pulse-plateau ripples and rise time remain the same as modules are added. All design goals are met except that the maximum pulse variation at the beginning of the pulse is 1.2 percent instead of the desired 1 percent. A drawback of this two-section module design is the rounded top of the 2 μsec pulse. A flatter pulse plateau would be desirable.

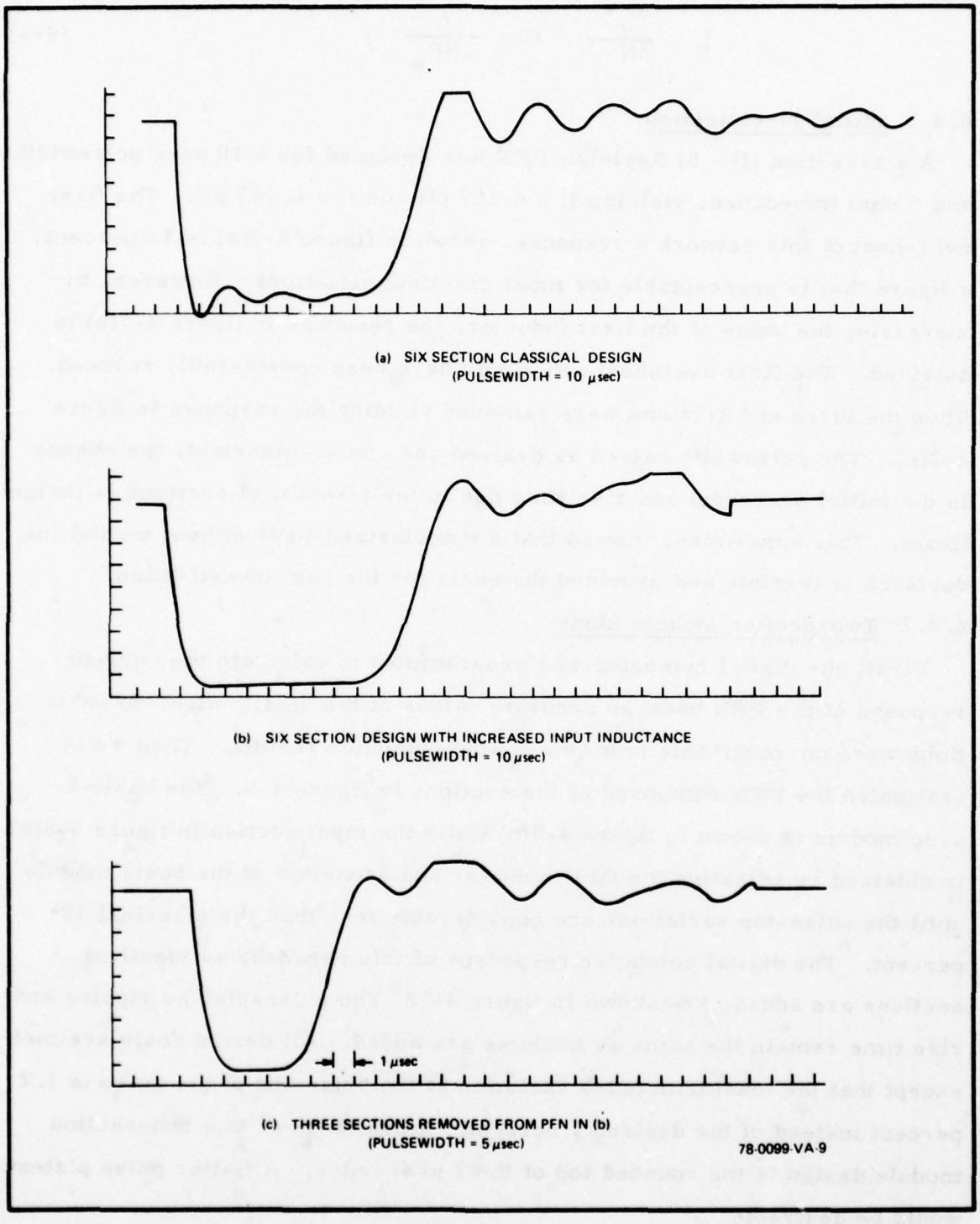

Figure 4-7. Current Pulses of Rayleigh PFN

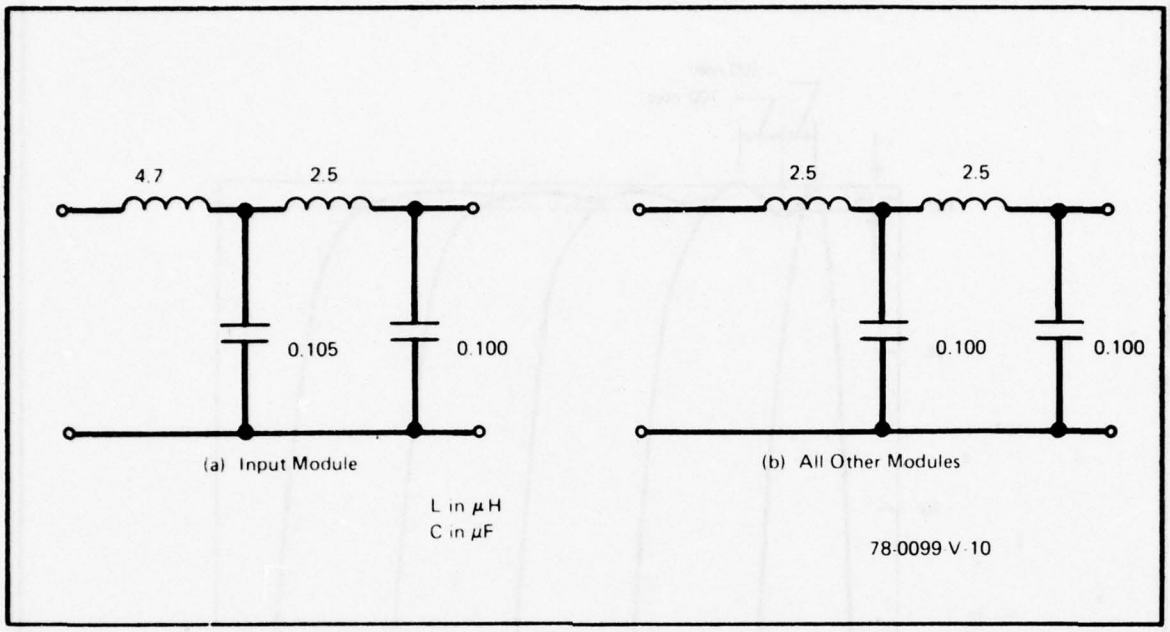

Figure 4-8. Two-Section Pulse Forming Modules

4.4.3 Three-Section Module Study

One design goal states that "any perturbations in amplitude within the 'flat' portion of the pulse will not have a rise time less than 500 nanoseconds." This restriction confines the two microsecond pulse to having no flat top at all, for any flattening of this pulse will require more than two sections and will result in a ripple half period of less than 500 nanoseconds. To verify this we designed the basic 2 μsec module in figure 4-10. The input module was obtained by adjusting the input inductor of the basic module until the pulse-top variation was nearly minimum. The responses of pulse forming networks composed of these modules are shown in figure 4-11. As expected, the pulse-top is broader at the expense of perturbation rise times less than 500 μsec.

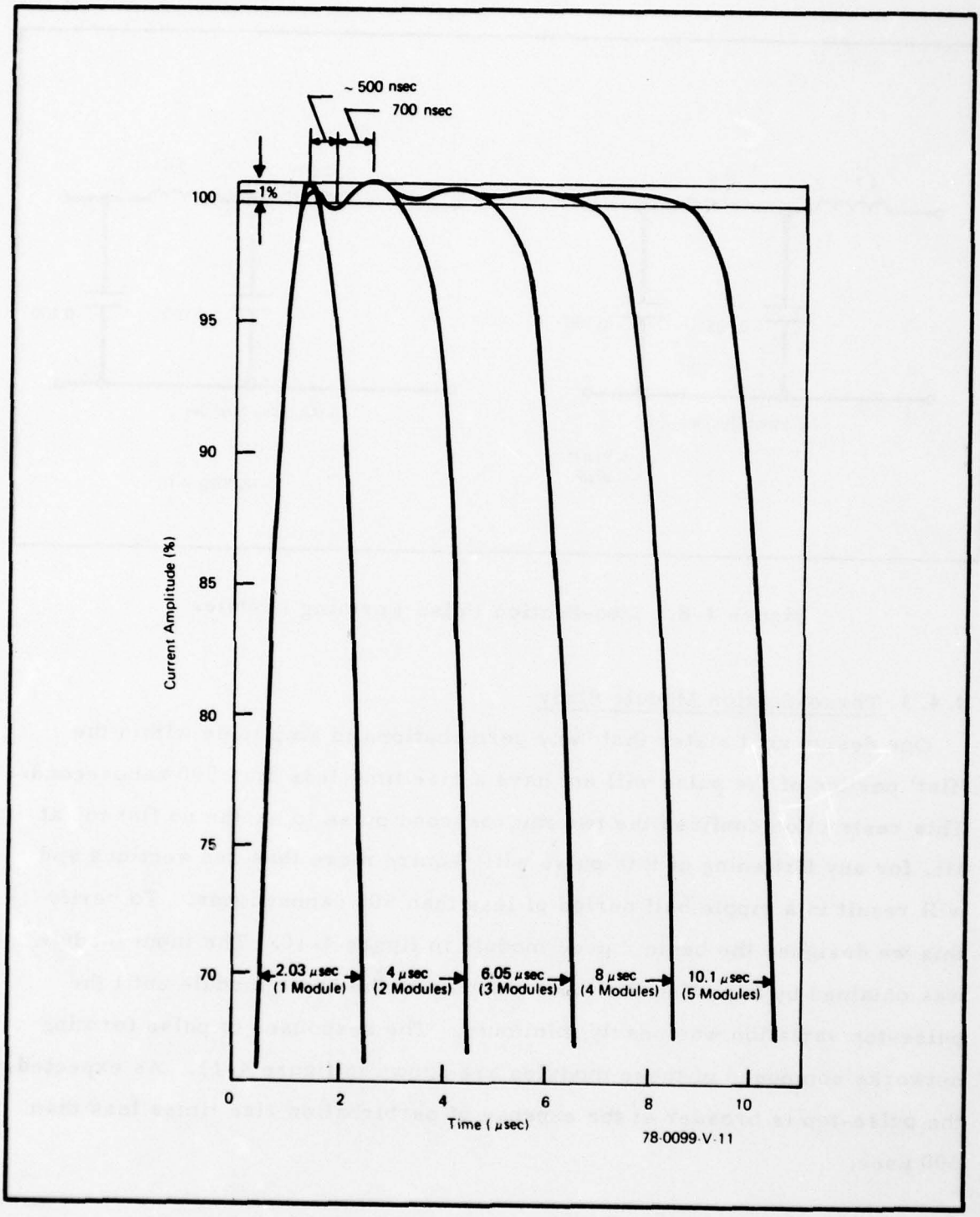

Figure 4-9. Pulse Responses of PFN in Figure 4-8

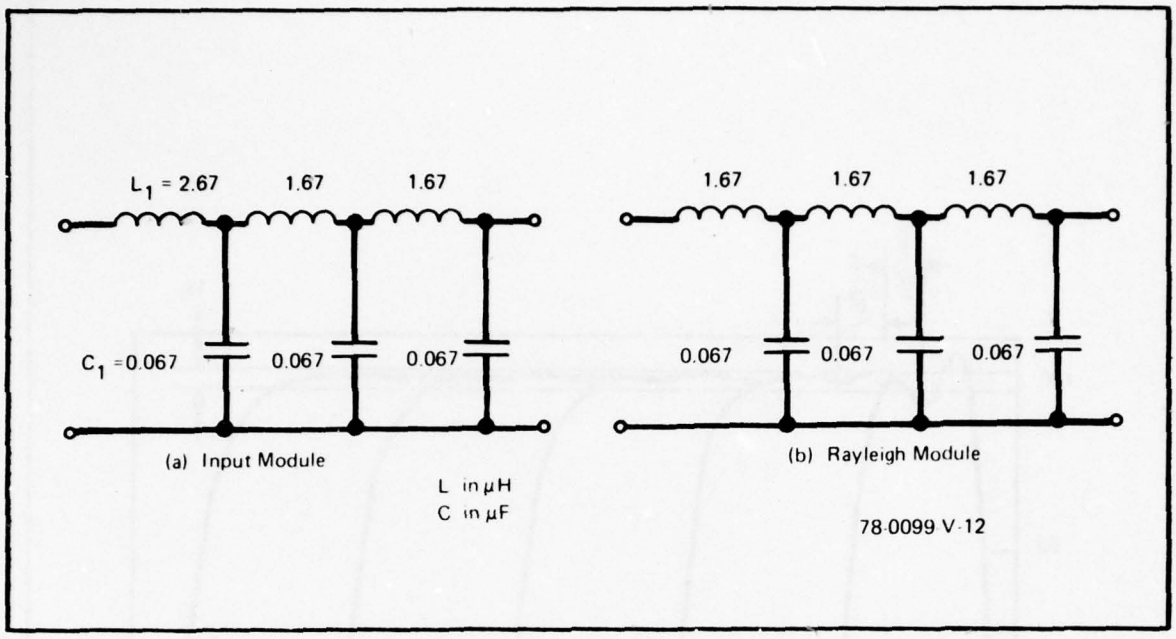

Figure 4-10. Three-Section Pulse Forming Modules

4.4.4 Perturbation Rise Time

The results of the two-section and three-section module studies showed that a tradeoff exists between pulse-top flatness and perturbation rise time. Discussions with the Program Technical Director during this study revealed that the first few perturbation rise times were not as important as those further down the pulse plateau. We now show the relationship among t_r, the rise time further down the pulse plateau, the pulsewidth τ, and the number of sections N.

After the initial high frequency transients die out, the pulse top can be approximated by a raised sine wave whose frequency is accurately given by

$$f_{rip} = \frac{1}{\pi\sqrt{LC}} \qquad (4\text{-}2)$$

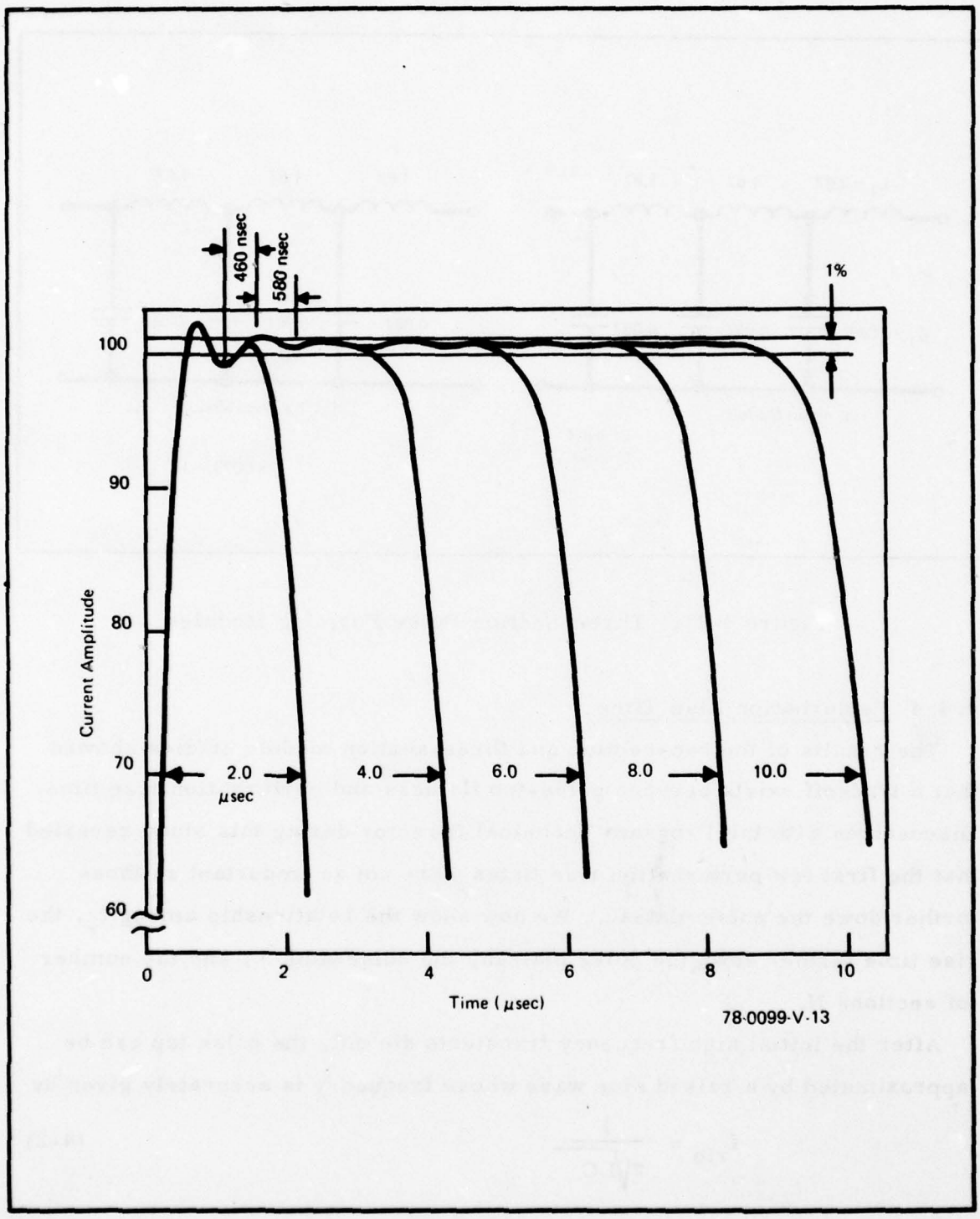

Figure 4-11. Pulse Responses of PFN in Figure 4-10.

where L and C are the Rayleigh network values in figure 4-3(b). The time for one cycle is

$$t_1 = \frac{1}{f_{rip}} = \pi\sqrt{LC} \qquad (4\text{-}3)$$

so the perturbation rise time is then

$$t_r = \frac{t_1}{2} = \frac{\pi\sqrt{LC}}{2} \qquad (4\text{-}4)$$

Substituting for L and C from equation (4-1) gives the perturbation rise time as

$$t_r = \frac{\pi\ \tau}{4\ N} \qquad (4\text{-}5)$$

For the desired pulsewidth of 2 μsec, t_r as a function of N is given in table 4-2. The values for N = 2 and 3 closely match the values obtained from figures 4-9 and 4-11, respectively. Only for N = 2 and 3 is t_r greater than the required 500 nanoseconds.

TABLE 4-2

t_r VERSUS N FOR A 2 MICROSECOND PULSE

N	t_r (nansec)
2	785
3	523
4	392

78-0099-TA-14

Since two sections do not yield a flat-top pulse, three sections were selected for the final module. The next part of the study was devoted to optimizing this section so that the pulse-top variation was 1 percent maximum.

4.4.5 Optimum Rayleigh Network

For the input section in figure 4-10, we showed in paragraph 4.4.3 that the pulse top variations could be considerably reduced by increasing the value of L_1. However, this one degree of freedom was not enough to reduce this ripple to the 1 percent goal so in this study phase we also varied C_1 (nominally 0.067 μF) to improve the response.

Computer responses in figure 4-12 show the interesting trends in the pulse-top response. For a fixed value of C_1, the initial overshoot decreases as L_1 increases, but the succeeding undershoot is relatively insensitive to this change. However, as C_1 is increased, this undershoot improves. Since the pulse rise time is proportional to L_1, it is also desirable that the value of L_1 be minimized. Consequently, the optimum parameters selected were $L_1 = 3.4$ μH and $C_1 = 0.073$ μF, and the corresponding pulse response is shown in figure 4-13. The ±0.5 percent variation has been achieved and the 2 μsec pulsewidth occurs very near the predicted 70 percent value. The significant aspect about this portion of the study is that the ±0.5 percent variation goal has been satisfied without incorporating mutual inductance between coils. The elimination of mutual inductance considerably eases the manufacture of the PFN. Figure 4-14 shows the optimum input module parameters and the Rayleigh module parameters.

The analysis in paragraph 4.4.3 showed that the cascade of the Rayleigh N = 3 modules with values L and C does not upset the initial portion of the pulse. This feature is again demonstrated in figure 4-13 which shows the response as one and then two N = 3 modules are added to the input module. The pulse-top variation remains within ± 0.5 percent and the desired pulsewidth again occurs near the 70 percent value. In this manner, an arbitrary

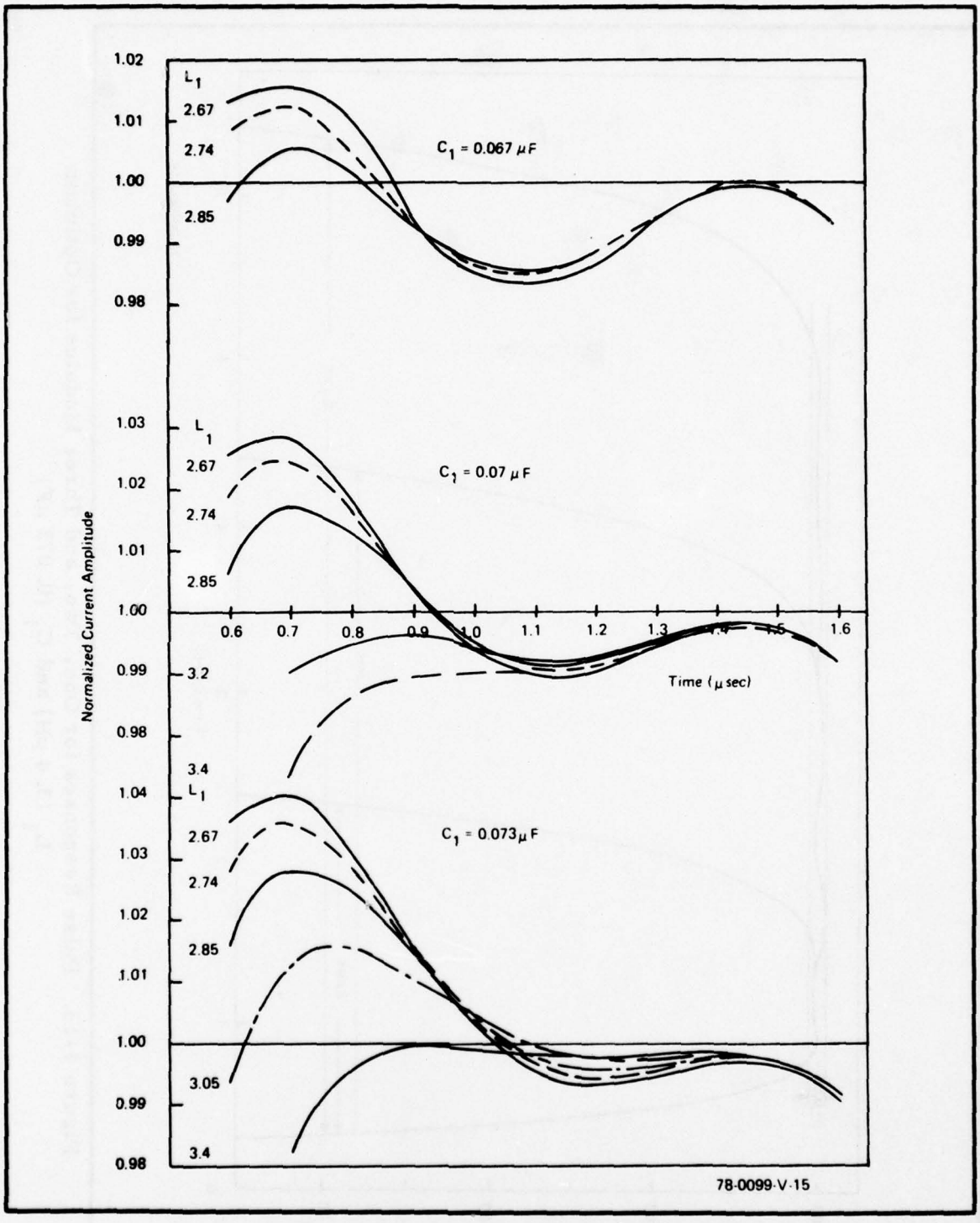

Figure 4-12. Pulse Responses About The Pulse Top As L_1 and C_1 Vary (N = 3 PFM in Figure 4-10(a)).

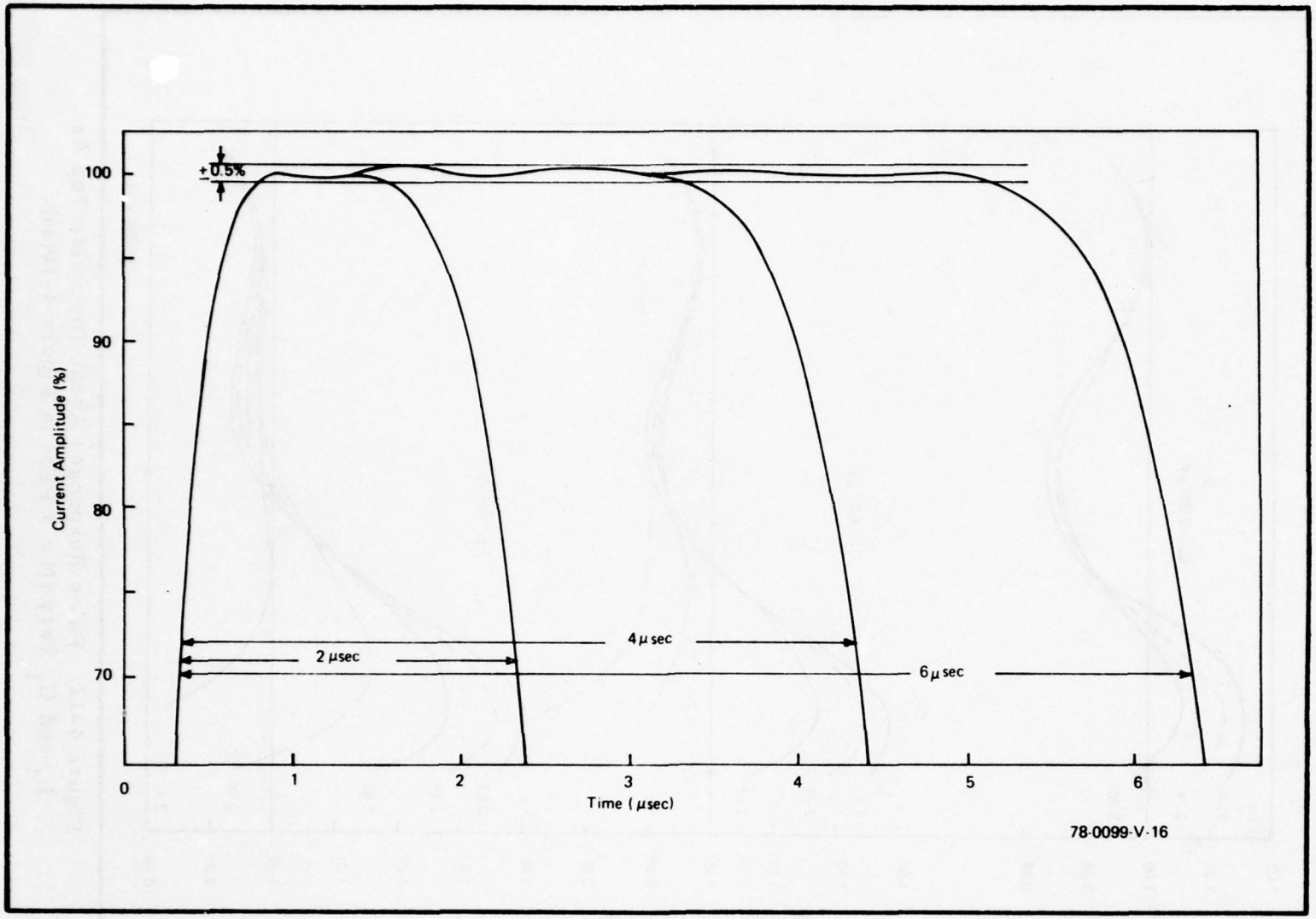

Figure 4-13. Pulse Responses for One, Two, and Three Modules for Optimum L_1 (3.4 μH) and C_1 (0.073 μF)

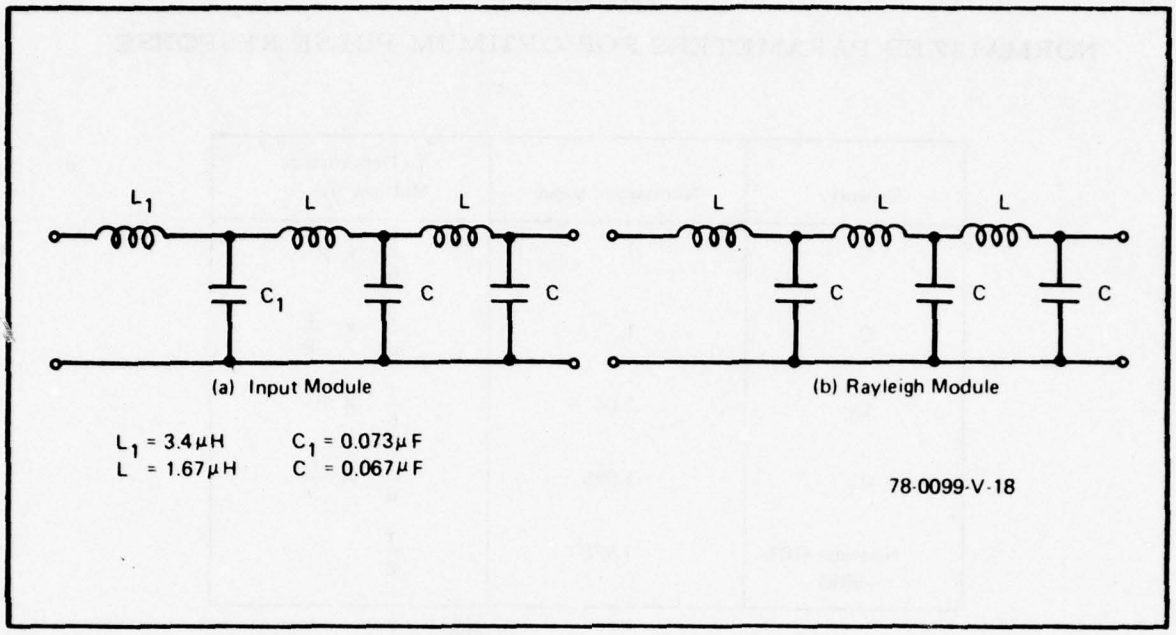

Figure 4-14. Optimum Pulse Forming Modules

pulsewidth can be achieved by the cascade of these identical basic building blocks. The commonality of these modules further reduces manufacturing cost and alignment time.

The optimum normalized parameters are presented in table 4-3. With these values the response in figure 4-13, for an arbitrary pulsewidth and impedance can be obtained. Use of this information allows a predictable response which includes the presence of the resistor R_o. This in itself is a major improvement over previous approaches, because the design procedures in [1] are based on an ideal voltage source ($R_o = 0$). Since there is no resistance in the circuit, the theoretical response is periodic. When the resistor R_o is included, the response degrades to a transient pulse that departs from the theoretical response. The above information eliminates this shortcoming of previously published design procedures.

TABLE 4-3

NORMALIZED PARAMETERS FOR OPTIMUM PULSE RESPONSE

Quantity	Normalized Value	To Denormalize Multiply by
L	1	$\frac{T}{6} \times R$
C	1	$\frac{T}{6} \times \frac{1}{R}$
L_1	2.04	$\frac{T}{6} \times R$
C_1	1.095	$\frac{T}{6} \times \frac{1}{R}$
Risetime (10% –90%)	1.428	$\frac{T}{6}$

78-0099-TA-17

4.5 SENSITIVITY STUDY

An important part of any network design is the response sensitivity to network parameter changes. Accordingly we examined the pulse-top response for changes in load resistor, the input inductor L_1, and the input capacitor C_1. Figure 4-12 shows the pulse-top response as L_1 and C_1 are changed. The strict tolerance of ± 0.5 percent for the response-top requires the tolerance of L_1 and C_1 to be approximately ± 2 percent.

In practice the load resistor is not always the design value R_o and this mismatch also alters the response. To determine this change we computed the response (L_1 = 3.3 μH, C_1 = 0.073 μF) for various values of the load resistor, and plotted them in figure 4-15. For a resistor change between +10 percent and -20 percent, the pulse-top variation remains within the 1 percent goal, although the peak current value changes.

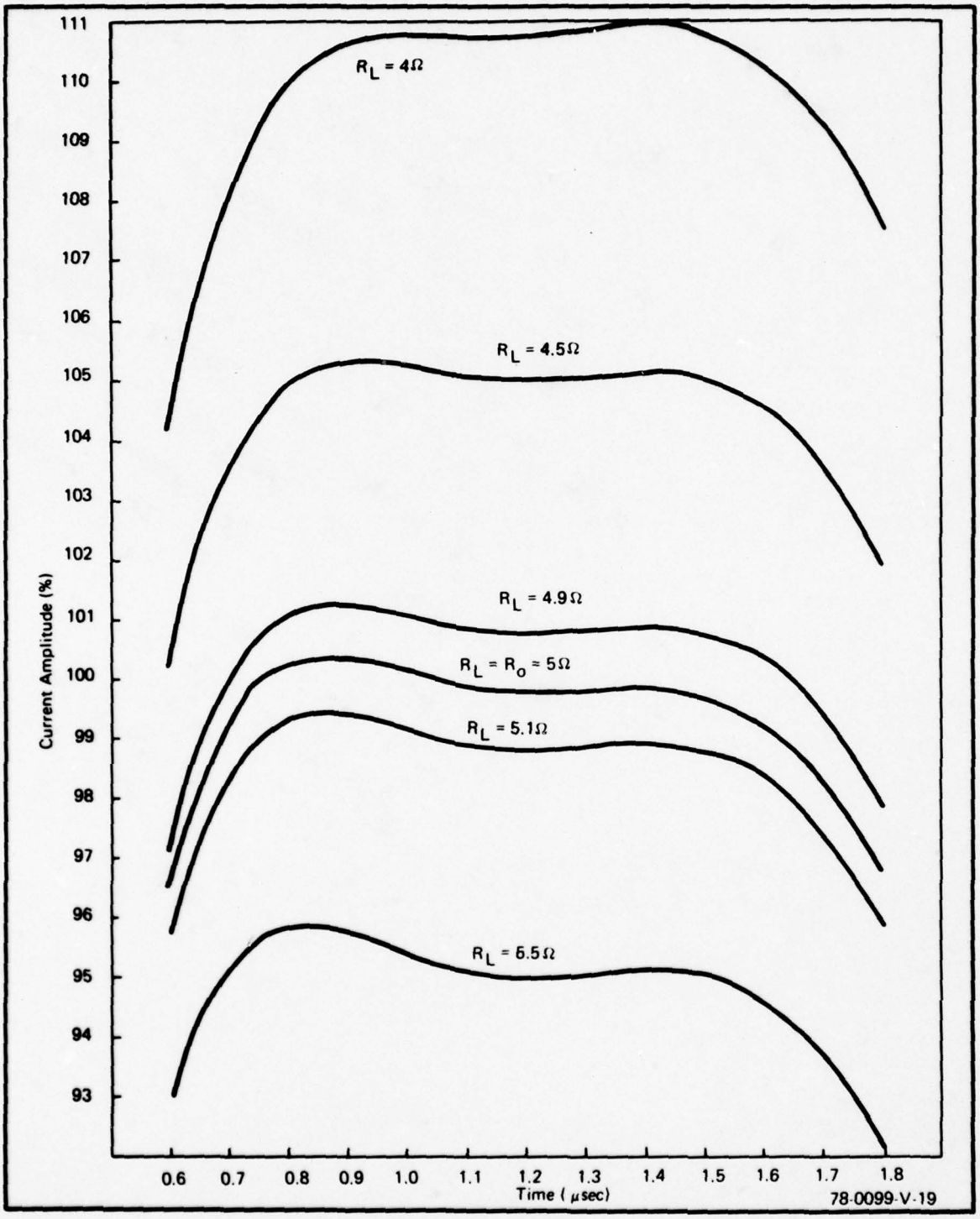

Figure 4-15. Pulse Forming Module Response as Load Resistor Varies

5. LOW-POWER BREADBOARD MODELS

Concurrent with the theoretical analysis, we assembled several low-power breadboard models to verify the modular concept, to verify that the optimum response could be realized in practice, to determine the effect of capacitor lead length, and to uncover any areas that could cause problems in the final high-power design.

5.1 VERIFICATION OF MODULAR CONCEPT

This 10-section breadboard PFN, shown in figure 5-1, had a 5Ω characteristic impedance and a 10 μsec pulsewidth. Each section was plug-in so that sections could be added or removed to change the pulsewidth. The element values of the input module and succeeding modules are given in figure 4-8.

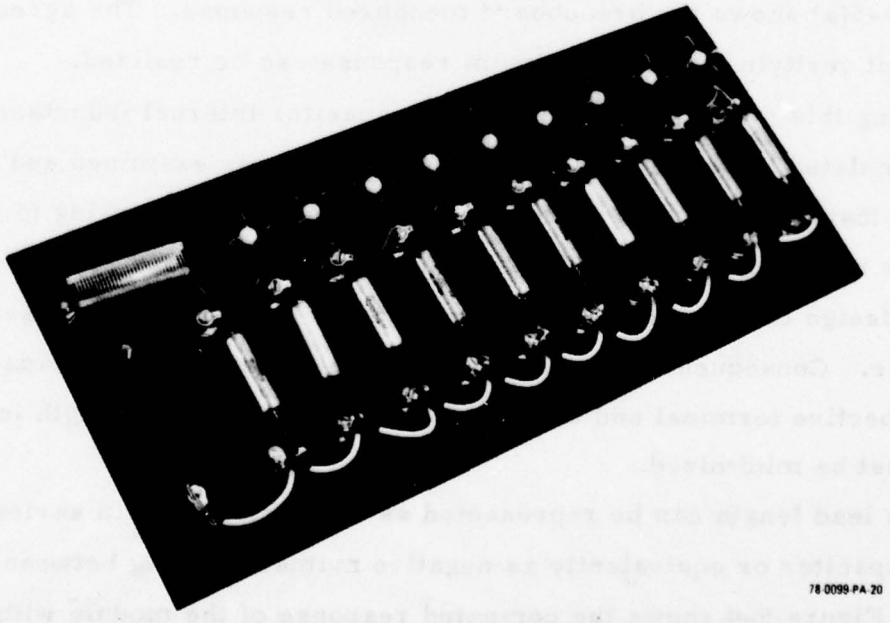

Figure 5-1. Low-Power Breadboard PFN for Verification of Theoretical Results

The capacitors were the CP09 type, which offers minimum inductance within the capacitor because of the extended foil construction. Each capacitor was measured to insure that the deviation from nominal was less than 5 percent. The first inductor was helix wound so that it could be tapped, thereby offering a variable inductor to compensate for element tolerances and to improve the response. All other inductors were wound on ferrite toroidal cores to minimize resistive losses. The responses as sections are added, shown in figure 5-2, verify that the modular concept is realizable in practice. The rise time and initial overshoot remain the same as the pulsewidth is changed.

5.2 OPTIMUM DESIGN AND LEAD LENGTH INVESTIGATION

A second low-power breadboard PFM was assembled to verify that the best theoretical response at that point in the study could be realized in practice. This 2-microsecond module, shown in figure 5-3, differs slightly from the final optimum module, whose input capacitor is 0.073 μF. In practice, however, this difference is not realizable owing to capacitor tolerances. Figure 5-4(a) shows this module's computed response and figure 5-5(a) shows the breadboard measured response. The agreement is excellent verifying that the optimum response can be realized.

During this study phase the effect of capacitor internal inductance, which was simulated by lead length in the breadboard, was examined and the results showed that this parasitic element changed the response, owing to the low network impedance (5Ω). This has important implications in the final high-power design because the three capacitors per module will be assembled in one case. Consequently connections must be made from each capacitor to its respective terminal and to ground, and this is the lead length in question that must be minimized.

This lead length can be represented as a inductance L_x in series with each capacitor or equivalently as negative mutual coupling between adjacent coils. Figure 5-4 shows the computed response of the module with an

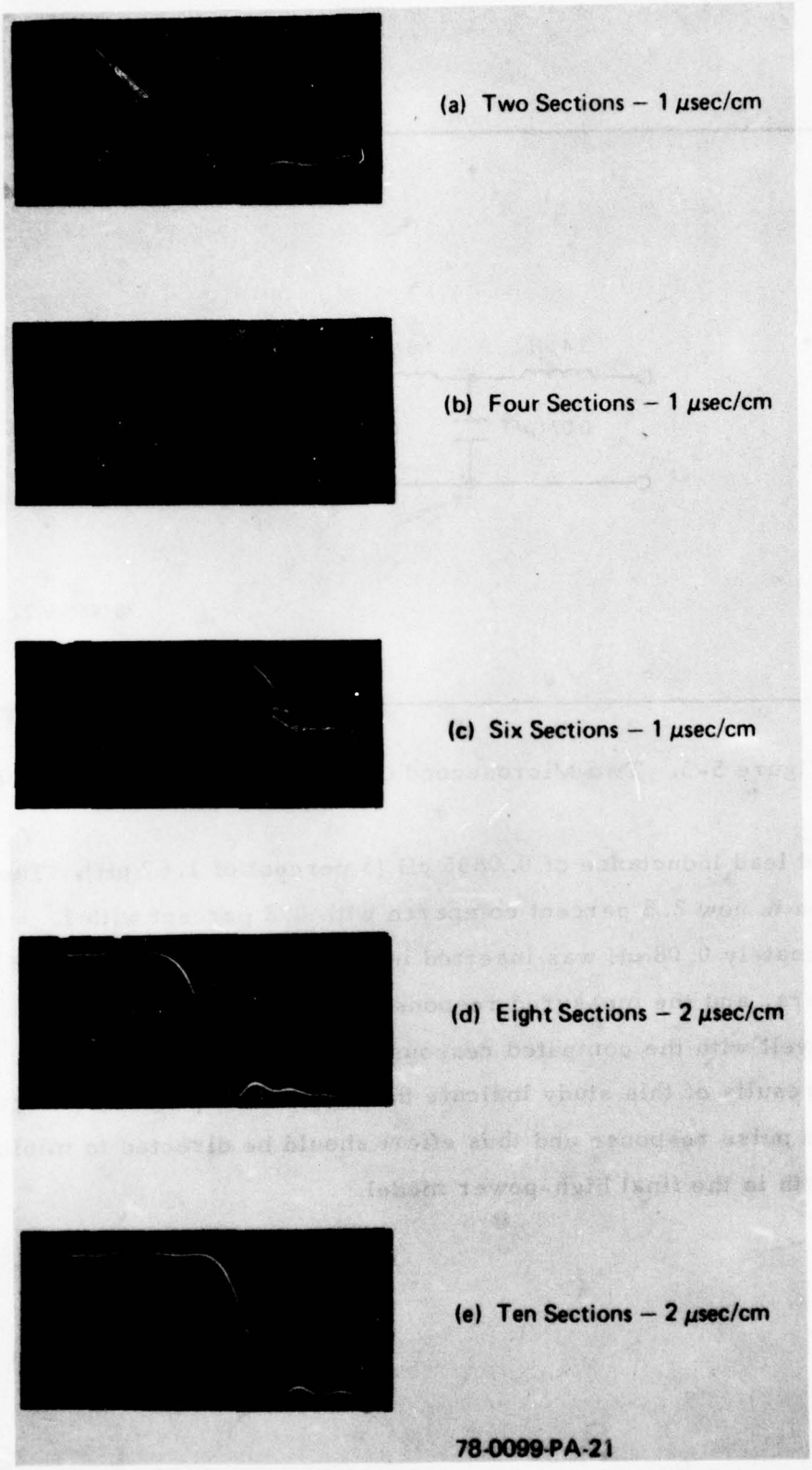

Figure 5-2. Response of PFN in Figure 5-1 as Sections are Added

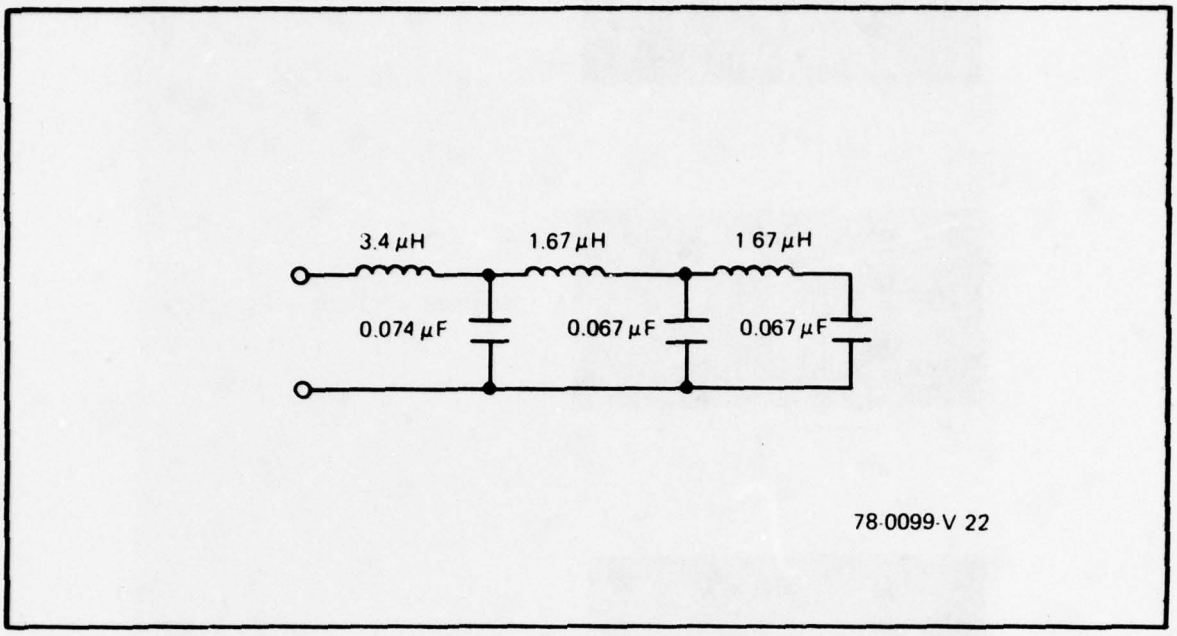

Figure 5-3. Two Microsecond Optimum Pulse Forming Module

assumed lead inductance of 0.0835 μH (5 percent of 1.67 μH). The peak deviation is now 2.8 percent compared with 0.2 percent with $L_x = 0$. Then approximately 0.08 μH was inserted in series with the breadboard PFM capacitors, and the measured response is shown in figure 5-5(b). Again it agrees well with the computed response.

The results of this study indicate that capacitor lead length degrades the optimum pulse response and thus effort should be directed to minimizing this length in the final high-power model.

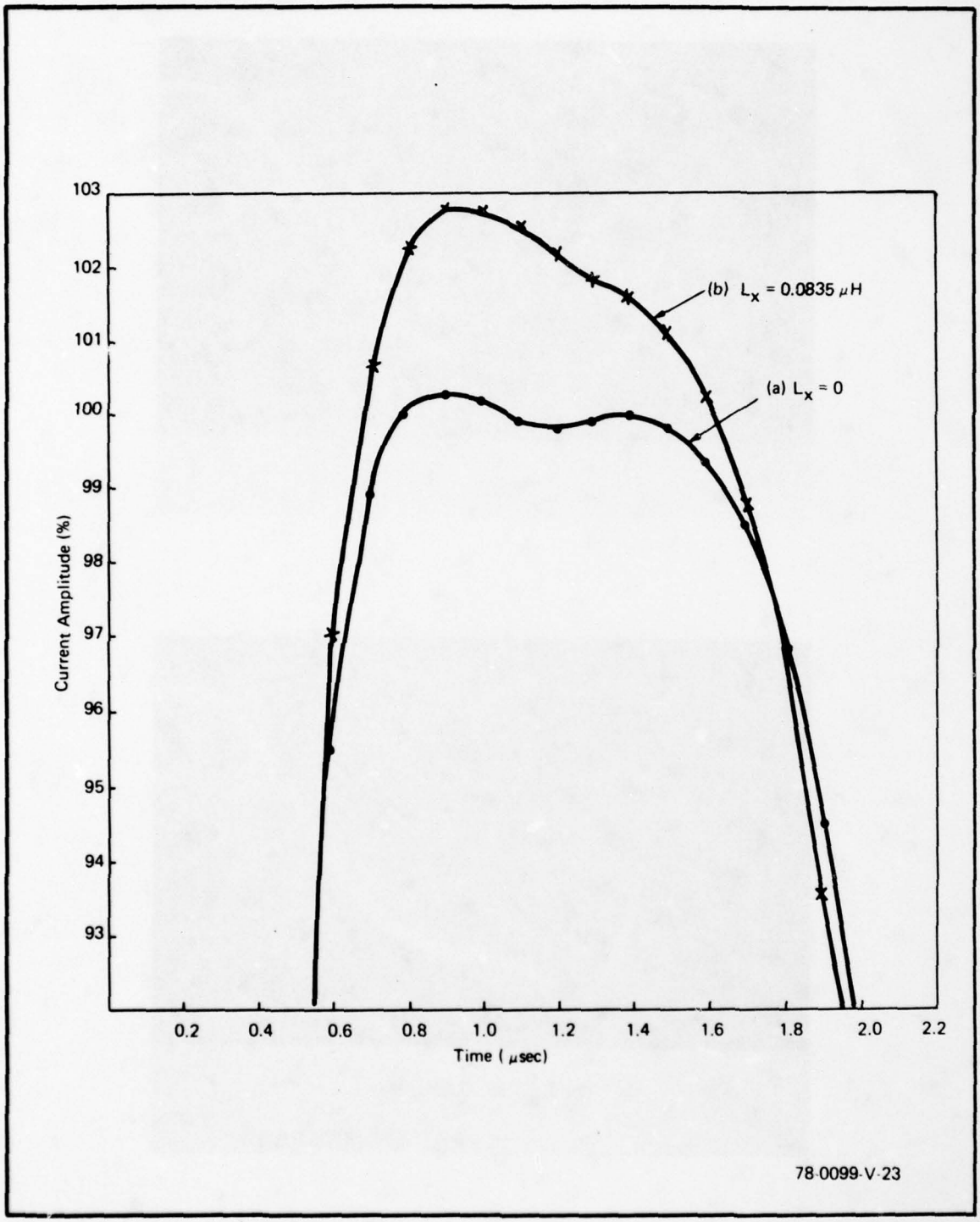

Figure 5-4. Computed Responses of PFN in Figure 5-3 Including Capacitor Lead Length Inductance L_x.

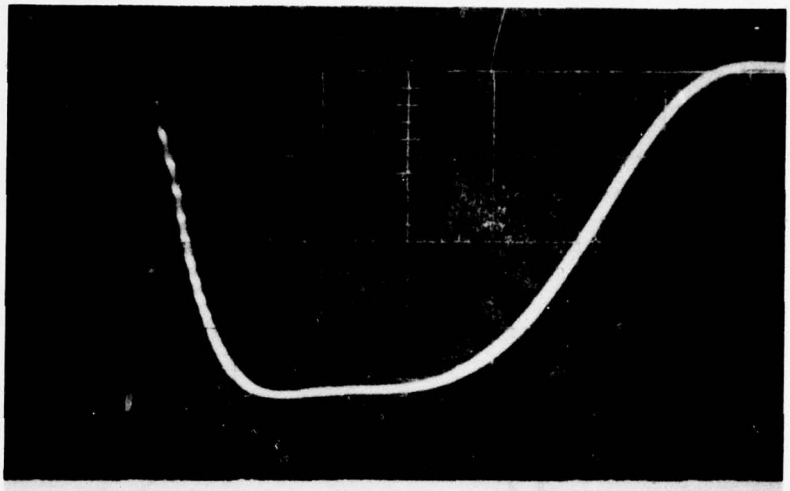

(a) $L_x \approx 0$

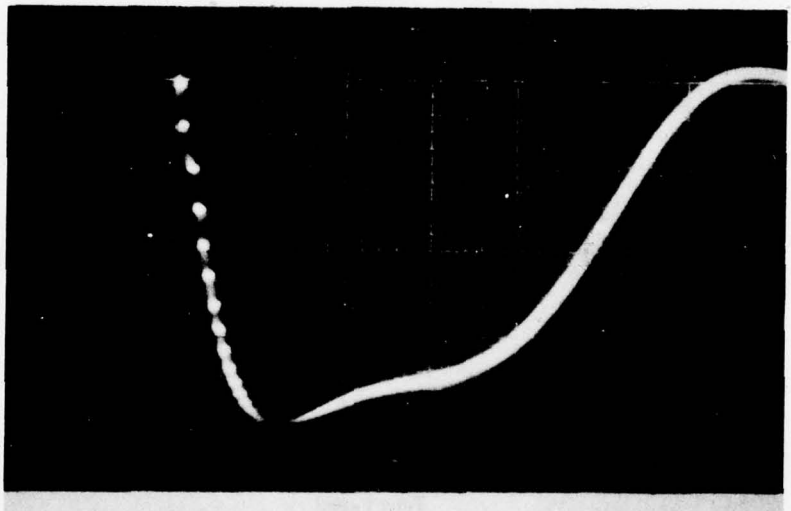

(b) $L_x \approx 0.08\mu H$

78-0099-PA-24

Figure 5-5. Measured Responses of PFN in Figure 5-4 Including Capacitor Lead Length Inductance L_x

6. HIGH POWER MODEL

Packaging of the high-power pulse forming module and the mating of these modules to form the final PFN require strict mechanical, electrical, and cost considerations to achieve the goals in section 2. The PFN must be rugged and be able to dissipate the generated heat, yet it is desired to have a minimum weight energy density of 2 joules/pound and a minimum volume energy density of 0.5 joules/cubic inch. Insulation to prevent arcing and minimum lead length to avoid parasitic inductance are important electrical considerations, while cost is important for large quantity manufacture. The capacitor assembly, coil construction, module assembly, and final tests are now discussed.

6.1 CAPACITOR ASSEMBLY

At the beginning of this program, simultaneous with the theoretical work, we sought information from outside suppliers and the Westinghouse Research and Development Laboratories on various capacitor arrangements for use in the PFM, with the goal being minimum size, weight, and cost. This survey showed that minimum size and weight would be achieved by packaging 3 paper-polypropylene oil dielectric capacitors in the same plastic container. This capacitor case would be 1.25 x 4 x 4 inches long and weigh 1.25 pounds. However, provisions for coil support and assembly would increase the overall dimensions to 6.875 inches high x 5.5 inches long x approximately 2.5 inches wide. The total weight per module would be 1.95 pounds.

6.2 COIL CONSTRUCTION

Two basic PFM packaging techniques are external coil and internal coil construction. In the internal coil construction, the entire PFM is enclosed in a metal container whereas the coil is exposed in the external coil

approach. The open-coil construction allows the windings to be forced-air cooled since they are exposed, thus offering the advantage of reduced overall size. The capacitors can be made independent of the coil configuration thereby providing a higher packaging density. On the other hand, the coil structure is not in the controlled environment that surrounds the internal coil. The internal coil offers better coil support and protection against shock and vibration. However, internal heat generated by the coils must be dissipated through the external area of the container and this aspect may cause a size increase. In general, much larger and heavier insulation bushings are used for the internal coil construction.

Since a main objective of this program was minimum size and weight, the external coil construction was selected for final packaging. This approach allowed experimental tests to be more easily performed since the exposed coils were then accessible.

The relatively small size of the capacitor assembly led to further consideration of the coil construction. The maximum RMS coil current, occurring in the first coil of the 10 μsec PFN, is

$$I_{RMS} = \sqrt{I_{Peak}\, I_{Aver}} = \sqrt{1000 \times 4} = 63 \text{ amp}$$

which dictates No. 8 copper wire. This large wire size leads to winding difficulties and results in a large coil size compared to the capacitor size. Therefore, we departed from conventional coil design and realized each coil as a spiral of enameled copper strap 0.365 x 0.032 inch on a 1-inch diameter form. Spacing between coils was approximately 2 inches to ensure negligible mutual coupling between coils. The coil assembly, supported by extensions of the capacitor case that contains the three module capacitors, was located directly above the capacitor terminals to ensure short lead lengths.

Initially, we found variations in conductor tension during coil winding, consequently inductance values did not remain within ±5 percent of the nominal value. However, we were able to easily control this inductance

value by applying a uniform tension to the conductor and then locking it in place with a plastic cable wrapped around the coil.

6.3 MODULE ASSEMBLY

The final assembly of the high-power module is shown in figure 6-1. Inductance and capacitance are within ± 5 percent of their nominal values. Off-the-shelf dry impregnated mica capacitors were used because the supplier could not meet the delivery schedule for polypropylene capacitors. The overall module dimensions were 2.75 inches wide x 4 inches high x 4 inches long. Note the extension of the capacitor case for coil mounting and the plastic cable wrapped around each coil to lock it in place.

Four holes in each side of the module and a bottom plate extension allow modules to be easily joined with screws, as shown in figure 6-2. A one-inch air spacing is allowed between adjacent modules for cooling, thus the length of a five-module assembly (10 μsec pulsewidth) is 17.75 inches. The design goal of 5 feet for the greatest dimension has been easily satisfied. Electrical connections between modules are made with No. 8 copper wire. The complete assembly is sufficiently rugged to withstand normal usage in a tactical radar system.

The densities for the PFM using polypropylene capacitors are computed as follows:

$$\text{Pulse Energy} = V_{peak} \times I_{peak} \times \text{Pulsewidth}$$

$$= 5 \times 10^3 \times 10^3 \times 2 \times 10^{-6} = 10 \text{ joules}$$

Therefore, the weight energy density is

$$W_D = \frac{10 \text{ joules}}{1.95 \text{ lb}} = 5.12 \text{ joules/lb}$$

and the volume energy density is:

$$V_D = \frac{10 \text{ joules}}{2.5 \times 6.875 \times 5.5 \text{ inches}} = 0.106 \text{ joules/in}^3$$

The weight energy density achieves the goal in section 2. The volume energy density was the best achievable with off-the-shelf capacitors. The

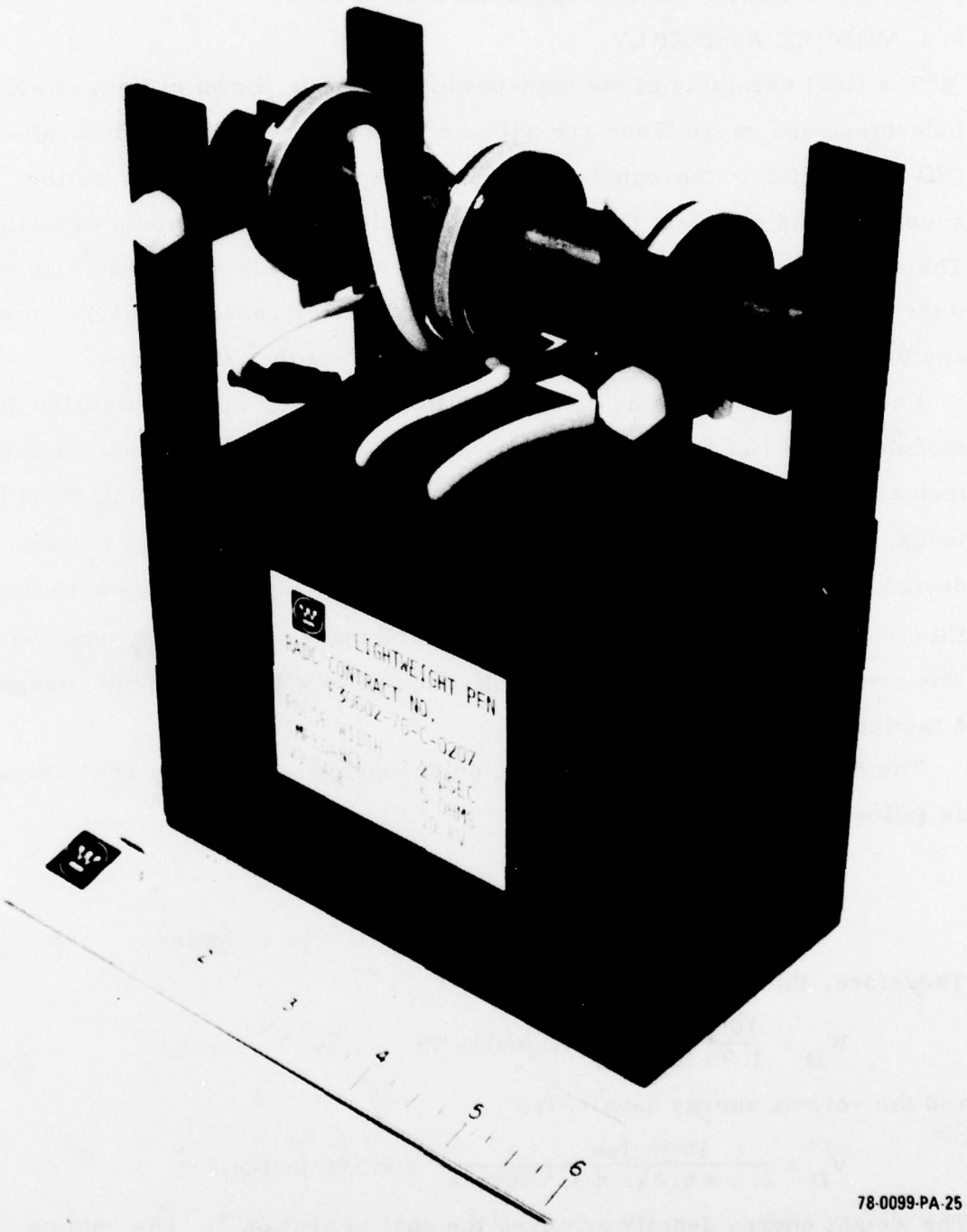

Figure 6-1. High-Power Pulse Forming Module - Final Model

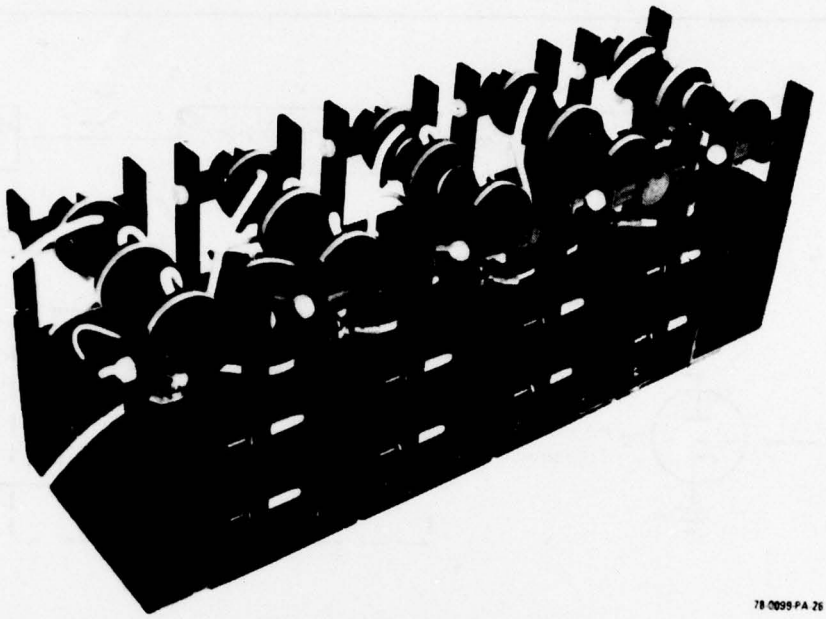

Figure 6-2. Pulse Forming Network Realized as a Cascade of the Pulse Forming Modules in Figure 6-1

goal of 0.5 joules/in^3 is not compatible with present state-of-the art components at these power levels.

6.4 HIGH-POWER TESTS

Here we describe the tests on the high-power model of the PFN as the pulsewidth is changed in 2 μsec steps. The basic module in these networks is shown in figure 6-1 and the pulsewidths were realized by stacking these modules as shown figure 6-2. All modules were the same except the input module, which had a larger input inductance and capacitance in accordance with the optimum design in figure 4-14.

The high-power test circuit, shown in figure 6-3, is a conventional line type modulator, composed of a variable voltage power supply, charging circuit, switch tube, and load resistor. The power supply had a voltage range from 0 to 7.5 kV and a maximum power capability of 1 kW. The charging circuit was a 0.5H inductor and a solid-state diode stack while the HY-5 thyratron acted as the discharge switch. Four 1.25 ohm air cooled

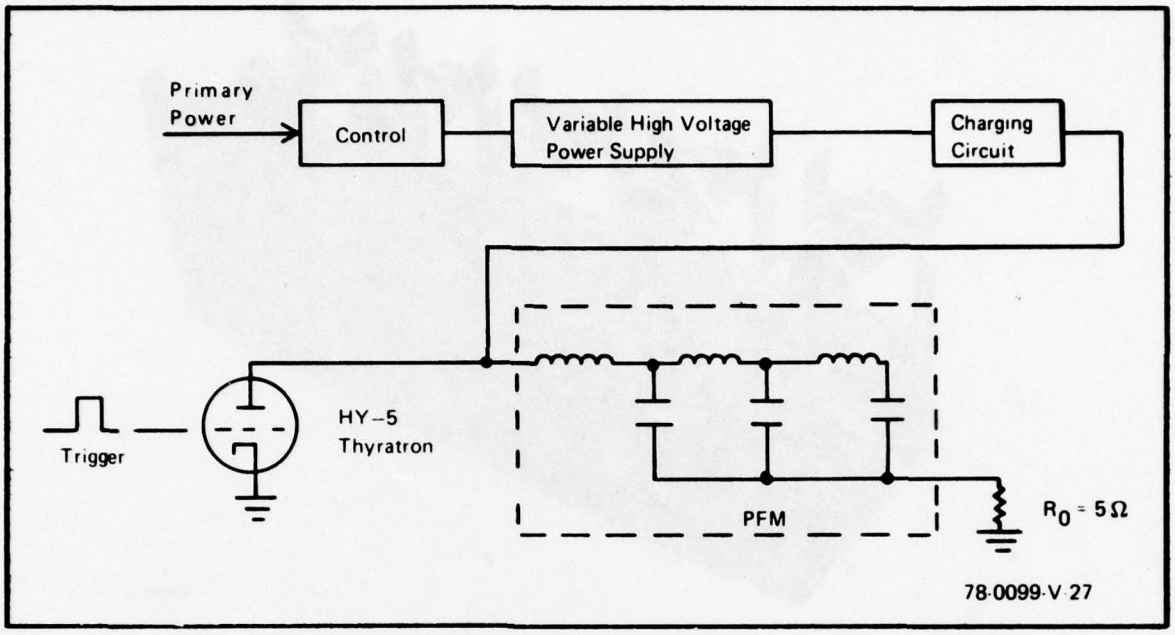

Figure 6-3. High-Power Test Circuit for the PFM

woven wire resistors connected in series provided a matched 10 kW load for the PFN test. The physical layout of the high-power test circuit required long leads, which added parasitic inductance. Therefore, we also determined a truer response at a low power level where stray inductance due to switch and load lead length could be minimized.

For the low-power tests, the thyratron switch was replaced by a mechanical vibrating switch, and the large 10 kW load was replaced by a small 4-watt resistor. All similar modules were randomly interchanged to prove that this maneuver caused negligible response change. Typical responses for two and five modules are shown in figure 6-4.

High-power testing was performed at 10 kV peak PFN storage voltage. Figure 6-5 shows the pulse responses for 1, 2, 3, 4, and 5 modules while table 6-1 gives the test results. The full peak and average power were met for 1, 2, and 3 modules. Laboratory power supply limitations required a reduced PRF for the 8 μsec and 10 μsec pulsewidths; however, the duty cycle

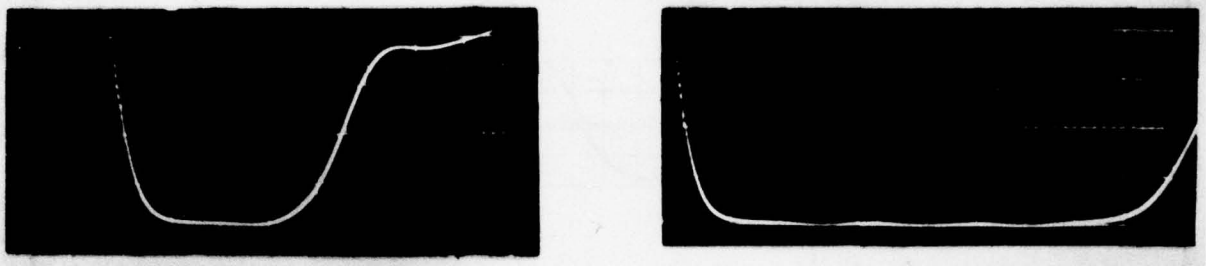

(a) 2 Modules

(b) 5 Modules

78-0099-PA-28

Figure 6-4. Low-Power Pulse Responses of Final PFN's (1 μsec/cm)

was maintained constant. The high frequency ripple on the pulse leading edge is stray pick up of the thyratron trigger and switching.

Although the same physical PFN was used for each low-power and high-power test, the responses are slightly different. As previously stated, this is due to the difference in test circuitry and instrumentation. With 2 modules the low-power waveform plateau is slightly rising, whereas the high-power waveform plateau is relatively flat. The 5-module high-power waveform has higher plateau ripple than the corresponding low-power waveform. The low-level test yielded a pulse plateau ripple of approximately ± 1.5 percent and gives a better indication of true PFN performance. The design goal of ± 0.5 percent ripple will be satisfied as component tolerance is improved.

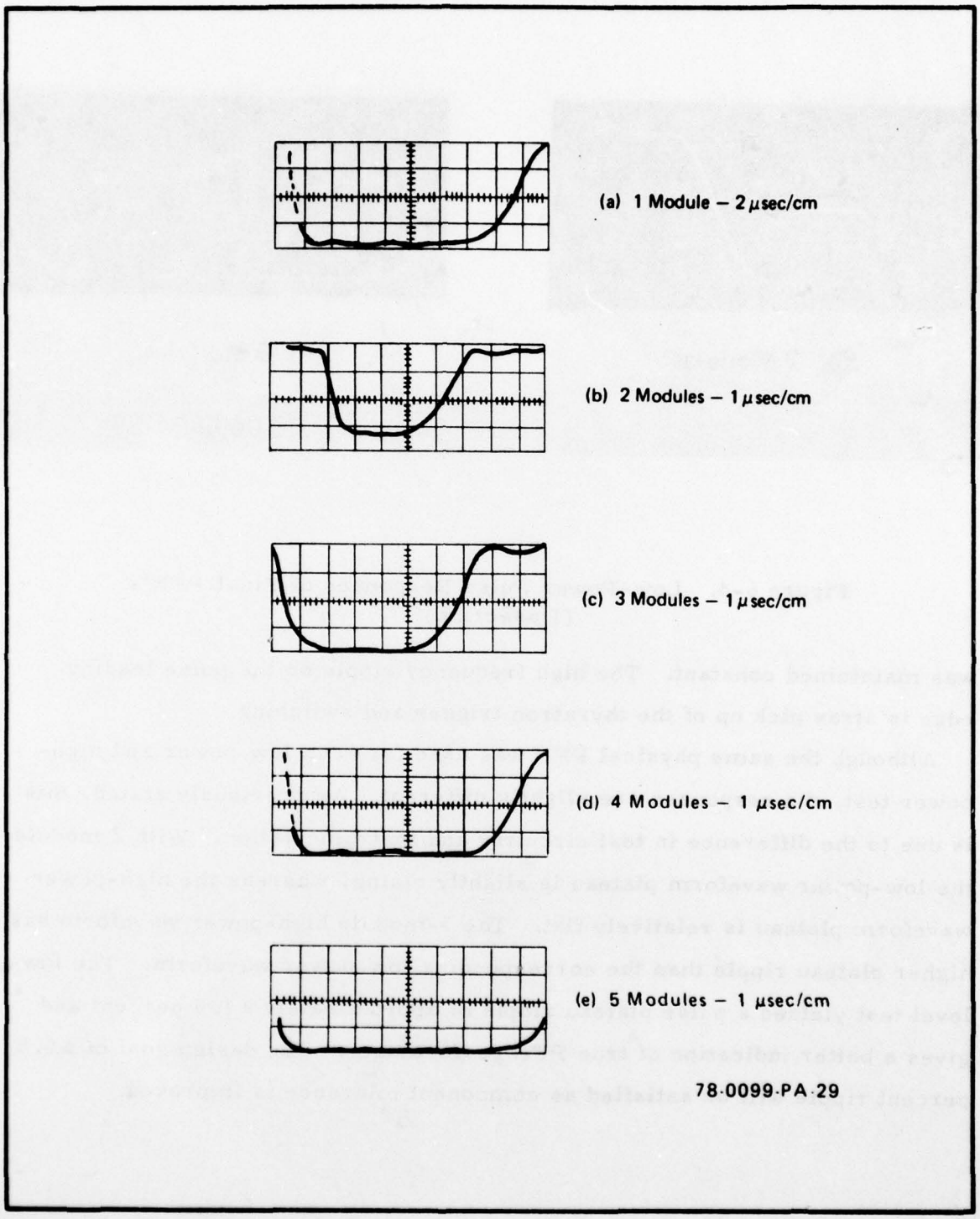

Figure 6-5. High-Power Pulse Responses of Final PFN's

TABLE 6-1

HIGH-POWER PFN TEST RESULTS

Parameter	Number of Pulse Forming Modules				
	1	2	3	4	5
Pulsewidth (μsec)	2	4	6	8	10
Peak Current (Amp)	1000	1000	1000	1000	1000
Average Current (Amp)	0.8	1.6	2.4	2.4	2.5
Peak Power (mW)	5	5	5	5	5
Charging Voltage (kV)	10	10	10	10	10
Rep.Frequency (pps)	400	400	400	300	250
Average Power (kW)	4	8	12	12	12.5

78-0099-TA-30

7. RECOMMENDATIONS FOR FUTURE STUDY

The development of a standard module combining the lightweight pulse forming module with integral charge and discharge circuits is a logical extension of the present program. This module will then be a basic modulator building block for a new family of modulators. The roadblock to developing this type of module in the past has been the inability to realize a modular PFN without mutual inductance as a design parameter. This restriction has now been lifted by the realization of the modular PFN described in this report.

This proposed standard module can be self-contained, needing only a power source and a trigger input. Cascading an appropriate number of modules establishes the desired pulse width. The peak power can be increased by adding modules in parallel. This approach also provides the capability for electronically varying the pulse width by selectively triggering appropriate modules since uncharged modules will not contribute to the pulse. This feature can be important for future generation military radars with ECCM capability.

Benefits of this modulator building block to the Air Force include reduced modulator acquisition cost, simplified logistics for maintenance, and versatility in synthesizing the transmitted pulse.

8. REFERENCES

1. Glasoe, G. N. and J. V. Lebacqz, Pulse Generators, Dover Publications, Inc., New York, N. Y., 1965. (This book was originally published as Volume 5 in the Massachusetts Institute of Technology Radiation Laboratory Series.)

APPENDIX A

Here we derive the characteristics of the distributed line given in table 4-1 based on the program requirements of

a. 5 megawatt peak pulse power

b. τ = 2 microsecond pulsewidth

c. R_o = 5 ohms characteristic impedance

The line under discussion is Case III in figure 4-2 and we now determine the required loss factor.

$$\alpha = R/L \tag{A-1}$$

where R is the line resistance and L is the line inductance, both per unit length. For illustrative purposes the total pulse droop over the full ten microsecond pulsewidth was assumed to be 10 percent, hence, the droop permitted per two microsecond module was 2 percent. With this restriction, the current after two microseconds (figure 4-2) must satisfy the inequality

$$1 - \frac{\alpha(2 \times 10^{-6})}{4} \geq 0.98 \tag{A-2}$$

or

$$\alpha \leq 4 \times 10^{4} \tag{A-3}$$

The impact of this value of α will be shown after we determine some intermediate quantities. The necessary transmission line equations for computing the total line capacitance C_T and total line inductance L_T are

$$\frac{\tau}{2} = \sqrt{L_T C_T} \tag{A-4}$$

$$R_o = \sqrt{\frac{L_T}{C_T}} \tag{A-5}$$

Simultaneous solution of (A-4) and (A-5) yields $C_T = 0.2\ \mu F$ and $L_T = 5\ \mu H$. The line length ℓ is

$$\ell = \frac{c}{\sqrt{\epsilon}} \times \frac{\tau}{2} = 649 \text{ ft} \qquad \text{(A-6)}$$

where $c = 9.843$ ft/sec is the speed of light and $\epsilon = 2.3$ is the dielectric constant of polyethylene, the line dielectric. For this line length, the capacitance per foot is

$$C = \frac{0.2 \times 10^{-6}}{649} = 308 \text{ pF/ft} \qquad \text{(A-7)}$$

and the inductance per foot is

$$L = \frac{5 \times 10^{-6}}{649} = 7.7 \times 10^{-3} \ \mu H/ft \qquad \text{(A-8)}$$

Then, from (A-1), (A-3), and (A-8)

$$R = \alpha L = 4 \times 10^{4} \times 7.7 \times 10^{-9} = 3.08 \times 10^{-4} \text{ ohms/ft} \qquad \text{(A-9)}$$

This is the DC resistance of a one foot long pair of copper conductors each having a resistance of 1.54×10^{-4} ohms/ft. This is equivalent to No. 2 wire, which has a cross-section area of 0.052 square inches. The total copper volume requirement for the two microsecond line is then

$$V = 0.052 \text{ in}^2 \times \frac{1 \text{ ft}^2}{144 \text{ in}^2} \times 2\ell = 0.469 \text{ ft}^3 \qquad \text{(A-10)}$$

The weight of this copper alone is 261 pounds since No. 2 wire weighs 0.201 pounds per foot. The energy in the 2 microsecond pulse is

$$E = P\tau = 5 \times 10^{6} \times 2 \times 10^{-6} = 10 \text{ joules} \qquad \text{(A-11)}$$

yielding energy densities of 0.0124 joules/in^3 and 0.038 joules/pound. Each is considerably less than the minimum design goals of 0.5 joules/in^3 and 2 joules/pound.

MISSION
of
Rome Air Development Center

RADC plans and conducts research, exploratory and advanced development programs in command, control, and communications (C^3) activities, and in the C^3 areas of information sciences and intelligence. The principal technical mission areas are communications, electromagnetic guidance and control, surveillance of ground and aerospace objects, intelligence data collection and handling, information system technology, ionospheric propagation, solid state sciences, microwave physics and electronic reliability, maintainability and compatibility.